EVALUATION OF THE CONSERVATIONAL CHANNEL EVOLUTION AND POLLUTANT TRANSPORT SYSTEM (CONCEPTS) APPLIED TO COMPOSITE STREAMBANKS IN THE OZARK HIGHLANDS ECOREGION

By

ERIN DALY

Bachelor of Science in

Biosystems Engineering

Clemson University

Clemson, South Carolina

2010

Submitted to the Faculty of the
Graduate College of the
Oklahoma State University
in partial fulfillment of
the requirements for
the Degree of
MASTER OF SCIENCE
December, 2012

EVALUATION OF THE CONSERVATIONAL CHANNEL EVOLUTION AND POLLUTANT TRANSPORT SYSTEM (CONCEPTS) APPLIED TO COMPOSITE STREAMBANKS IN THE OZARK HIGHLANDS ECOREGION

Thesis Approved:

Dr. Daniel E. Storm

Thesis Adviser

Dr. Garey A. Fox

Dr. Donald J. Turton

Name: ERIN DALY

Date of Degree: DECEMBER, 2012

Title of Study: EVALUATION OF THE CONSERVATIONAL CHANNEL EVOLUTION AND POLLUTANT TRANSPORT SYSTEM (CONCEPTS) APPLIED TO COMPOSITE STREAMBANKS IN THE OZARK HIGHLANDS ECOREGION

Major Field: BIOSYSTEMS ENGINEERING

ABSTRACT: The objectives of this study were to perform an evaluation of the Conservational Channel Evolution and Pollutant Transport System (CONCEPTS) applied to composite streambanks in the Ozark Highlands ecoregion, and to demonstrate CONCEPTS's ability to predict the long-term stability of streambank stabilization. In order to accomplish these objectives, CONCEPTS was used to simulate a 9.25 km reach along the Barren Fork Creek in Northeastern Oklahoma. A sensitivity analysis was first performed to identify input parameters with the greatest effect on bank erosion predictions in CONCEPTS. The alpha correction factor and the internal angle of friction of the bank soils were found to be the most sensitive followed by the critical shear stress, effective cohesion, erodibility coefficient and the permeability. Next, CONCEPTS was calibrated using ground-based and aerial bank retreat measurements to produce realistic processes and predictions. Model calibration was conducted by reducing the critical shear stress of the noncohesive soils until the predicted retreat matched the observed data. Using the calibrated model, two streambank stabilization techniques were simulated at two highly unstable cross sections. Fluvial erosion was reduced by simulating the application of riprap at the bank toe, and geotechnical failure was reduced by simulating a slope stabilization technique. In general, CONCEPTS predicted a high percent reduction of cumulative fines yield, bank retreat at the bank top and toe, and cumulative change in thalweg elevation for both stabilization techniques. Due to CONCEPTS limitations, a two or three-dimensional model is needed to perform a comprehensive analysis of streambank stability for the composite streambanks in the Ozark Highlands ecoregion. Additional research is needed on the use of the internal angle of friction as a lumped calibration parameter. However, with the proper calibration and caution, CONCEPTS is a useful tool to guide the design and prioritization of streambank stabilization projects.

TABLE OF CONTENTS

LIST OF TABLES

LIST OF FIGURES

CHAPTER I

INTRODUCTION

The State of Oklahoma is home to a great variety of valuable water resources. However, changes in land use, riparian degradation, and channel alterations are proving to be a considerable threat to many of Oklahoma's surface waters. This study focuses on the Illinois River basin, one of the state's high priority basins in northeastern Oklahoma. The basin has some of the state's most treasured streams and rivers as well as Tenkiller Ferry Lake, an important reservoir that serves as the drinking water source for a large portion of that region. The basin is also home to designated scenic rivers that are protected for their unique natural scenic beauty and recreational values. This has created a thriving recreational and tourism industry that attracts thousands of visitors to the basin each year.

1.1. Background

The Illinois River basin covers 4,330 km^2 spanning the northeastern Oklahoma-Arkansas border. Approximately 54% of this basin is located within Oklahoma. The Illinois River, the principle stream for the basin, drains into Tenkiller Ferry Lake (Figure 1-1). The basin falls within the Ozark Highlands ecoregion, which typically contains

streams that are riffle and pool dominated, clear, and have coarse gravel, cobble, or bedrock substrates. Banks are typically composite and include a silty loam top layer with an unconsolidated gravel bottom layer and toe. The dominating land uses in the basin are forest and hay production or pasture with the major agricultural industry being poultry and cattle (OCC, 2010).

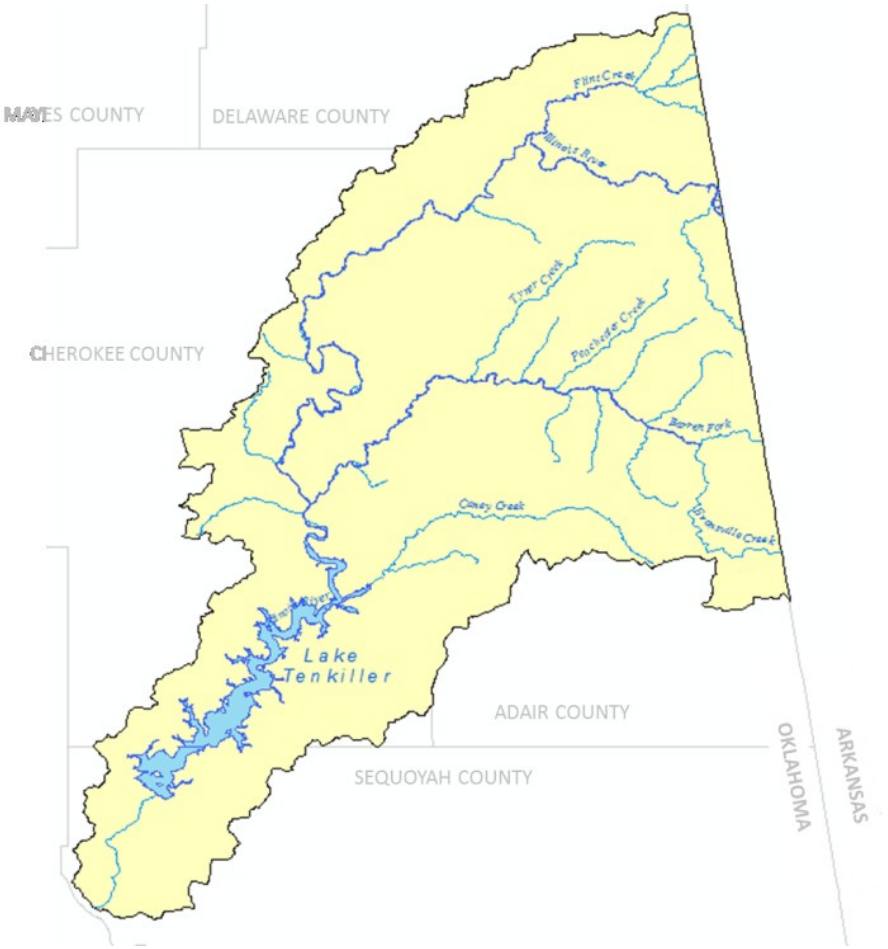

Figure 1-1. The Illinois River basin (Oklahoma only).

Historical data indicate good water quality in the Illinois River basin up to the early 1970s. After this time nutrient loading and eutrophication became, and continues to be, an issue. The annual Oklahoma 303(d) list for impaired and threatened waters generally states phosphorus, bacteria, and sediment as the impairment causes for the

waters in this basin (OCC, 2010). The Illinois River basin also includes three of the state's six designated Scenic Rivers: Illinois River, Flint Creek, and Barren Fork Creek. These streams have experienced similar declines in water quality despite their more rigorous standards and protection.

Streambank erosion is known to be a significant source of sediment in many impaired streams (Simon et al., 2000; Cancienne et al., 2008; Fox and Wilson, 2010). These streambank sediments are often higher in nutrients as well, contributing to the nutrient loading of the stream. Streambank stabilization procedures and restoration designs have recently received a great deal of attention in order to help combat this issue (Shields et al., 2003). Stabilization projects have long-term, profound impacts on the entire stream corridor, so selecting the appropriate design and site for implementation is critical.

1.2 Objectives

Hydraulic models are often employed to predict the response of a stream to a proposed restoration design. The shortfall of many currently used models is that they only look at the site where stabilization will occur without considering upstream and downstream effects. The Conservational Channel Evolution and Pollutant Transport System (CONCEPTS) works to combat this shortcoming by modeling flow, sediment transport, and bank stability on a reach scale (Langendoen, 2000). The ability of this model is attractive to basin managers; however, CONCEPTS is still an emerging model and has not been applied to a wide variety of composite streambanks that include both cohesive and noncohesive soil layers. Therefore, the objective of this study was to perform an evaluation of CONCEPTS applied to composite streambanks in the Ozark Highlands ecoregion and assess CONCEPTS ability to model long-term streambank stabilization on these composite banks.

In order to accomplish this objective, CONCEPTS was used to simulate a 9.25 km reach along Barren Fork Creek. The study was divided into three sub-objectives as follows:

1. Perform a sensitivity analysis to identify input parameters that have the greatest effect on bank erosion predictions in CONCEPTS.
2. Perform a CONCEPTS model calibration using the information from the sensitivity analysis to produce realistic processes and predictions.
3. Perform an analysis of typical streambank stabilization procedures that address fluvial erosion and geotechnical failures using CONCEPTS. Demonstrate the ability of CONCEPTS to predict long-term success or failure of stabilization projects.

CHAPTER II

BACKGROUND AND REVIEW OF LITERATURE

Natural channel systems are complex and dynamic. This study focuses on an analysis of streambank morphology and resulting channel morphology over time. By understanding the processes of the streambank erosion, in terms of typical driving and resisting forces, a physically accurate model can be constructed to understand the channel evolution over time and therefore aid in recommendations for better management decisions and restoration designs.

2.1 Channel Morphology

Simon (1989) developed a six-stage, process-oriented channel evolution model for disturbed alluvial channels. The evolution model is a cyclical process of bank retreat and bank-slope development that occurs until an equilibrium, or stable channel state, is reached. Stage I, or the pre-modified stage, is assumed to be the natural, stable channel with low angle banks and established vegetation. Stage II, the constructed stage, is generally a man-made trapezoidal channel solely for the purpose of maximum conveyance and is the transition between stable and unstable channels. Stages III and IV, the degradation and threshold stages, are the two unstable stages in which erosion

of the bed and banks occurs in a cyclical process. Stage V, the aggradation stage, occurs when aggradation occurs on the channel bed; however, the bank heights in this stage still exceed critical values causing the banks to still be unstable and bank erosion continues to occur. Stage VI, the restabilization stage, shows a reduction in bank heights by aggradation on the channel bed and a decreased amount of bank erosion.

Stages III, IV, and V encompass the stages in which the channel continues to evolve and migrate through processes of aggradation and degradation. Degradation results from bed scouring, fluvial erosion, and geotechnical failures from the streambanks, while the aggradation results from sediment deposition from degradation upstream. These processes are exaggerated on river bends where additional energy along the outside of the bend may cause more degradation and reduced energy on the inside of the bend may cause more aggradation (Crosato, 2009). In order to understand the degradation, a closer look at bank morphology is needed.

2.2 Bank Morphology

Streambank erosion, or degradation, can be separated into two main categories based on the governing mechanism: fluvial erosion or mass wasting due to geotechnical failures. Fluvial erosion occurs when excess shear stress applied to the bank by the water flow provides enough force to detach and entrain particles from the bank. Fluvial erosion is often characterized by a critical shear stress, the amount of shear needed in order to detach bank material, and an erodibility coefficient that describes how fast the material is detached once the critical shear stress has been reached. This is a continuous process with time as long as the critical shear stress is exceeded. Geotechnical failures, however, are episodic and occur when the driving forces in the bank exceed the resisting forces causing an unstable condition and a block of material to detach from the bank. The stability of the bank is most often characterized using a factor

of safety (*FS*) approach, which uses the ratio of the resisting forces to the driving forces. If the *FS* is greater than one, the bank is stable as the resisting forces are greater than the driving forces. If the *FS* is less than one, a bank failure will occur on the most critical potential failure surface causing a portion of the bank to collapse and thus a mass failure. Driving forces within the streambank are due to gravity and the weight of the failure block, while resisting forces are the friction and cohesion of the bank material that resist movement (Langendoen, 2000).

2.3 Streambank Stabilization

The purpose of a streambank stabilization project is to slow or stop degradation processes from occurring at certain points along a stream reach. Therefore, both fluvial and geotechnical failures should be addressed when designing a stabilization project. Fluvial erosion is typically combatted with hard armoring at the bank toe or a realignment of the stream's energy. Riprap, for example, may be applied to the toe of a streambank to offer an increased resistance to fluvial erosion. The selected riprap will have a much higher critical shear stress and much lower erodibility coefficient, and therefore can withstand much larger flows than the natural bank material. Rock vanes may also be used to achieve a similar affect. By redirecting the flow's energy into the center of the channel and away from the bank, a reduced amount of shear stress is applied to the streambank, resulting in reduced fluvial erosion (FISRWG, 1998).

Mass wasting by geotechnical failure can be combatted in a variety of ways as well. Sloping of the banks decreases the bank heights which reduces the driving force of gravity on the bank, thereby resulting in fewer geotechnical failures over time. Instead of reducing the driving forces within the bank, the resisting forces can also be increased through vegetative plantings. Root systems create added cohesion to the bank, which increases the resisting forces and decreases failures due to mass wasting. Both

geotechnical and fluvial processes can be addressed when designing a stabilization project, with the focus on altering the resisting and driving forces on the bank (FISRWG, 1998).

2.4 Model Backgrounds

Three separate models, a primary model with two supporting models, were used in this study to simulate streambank erosion. The Conservational Channel Evolution and Pollutant Transport System (Langendoen, 2000) was the primary model utilized to simulate the physical processes of the reaches. The RVR Meander model (Abad and Garcia, 2006) was a supporting model used to simulate channel migration over time and to quantify the increased shear stress on channel bends. Finally, the Bank Stability and Toe Erosion Model (Simon et al., 2001) was the second supporting model as the precursor to the main model, and was used to estimate unknown soil parameters.

2.4.1 Conservational Channel Evolution and Pollutant Transport System

The Conservational Channel Evolution and Pollutant Transport System (CONCEPTS), developed by the United States Department of Agriculture Agricultural Research Services (USDA-ARS), simulates unsteady, one-dimensional flow, graded sediment transport, and bank erosion processes on a reach-scale in stream corridors (Langendoen, 2000). CONCEPTS simulates these processes through the use of three sub-models: hydraulics, sediment transport and streambed adjustment, and bank erosion and stream width adjustment.

The hydraulics sub-model assumes unsteady, one-dimensional open-channel flow along the centerline of the channel, and uses a distributed flow routing method to compute the flow as a function of time simultaneously at each cross section being modeled. The governing equations for this sub-model are the Saint Venant equations

consisting of a continuity equation and a momentum equation. The continuity equation used is:

$$B\frac{\partial y}{\partial t}+\frac{\partial Q}{\partial x}=q \tag{2.1}$$

where *B* is flow top width (m), *y* is stage (m), *t* is time (s), *Q* is discharge (m^3/s), *x* is distance along the channel (m), and *q* is the lateral flow into the channel, such as groundwater or overland flow, per unit length of channel (m^2/s). The momentum equation reads:

$$\frac{\partial Q}{\partial t}+\frac{\partial}{\partial x}\left(\frac{Q^2}{A}\right)+gA\left(\frac{\partial y}{\partial x}+S_f\right)=0 \tag{2.2}$$

$$S_f=\frac{n^2Q^2}{A^2R^{2/3}} \tag{2.3}$$

where *A* is flow area (m^2), *g* is gravitational acceleration (m^2/s), S_f is the friction slope (m/m), *n* is Manning roughness coefficient, and *R* is the hydraulic radius (m) (Langendoen, 2000).

This set of the Saint Venant equations is known as the dynamic wave model. If the inertia terms in Equation 2.2 are neglected, the set of equations is known as the diffusion wave model. Depending on the conditions being simulated, CONCEPTS automatically switches between the dynamic and diffusion wave models. Figure 2-1 provides a visual of the hydraulic variables used in this sub-model.

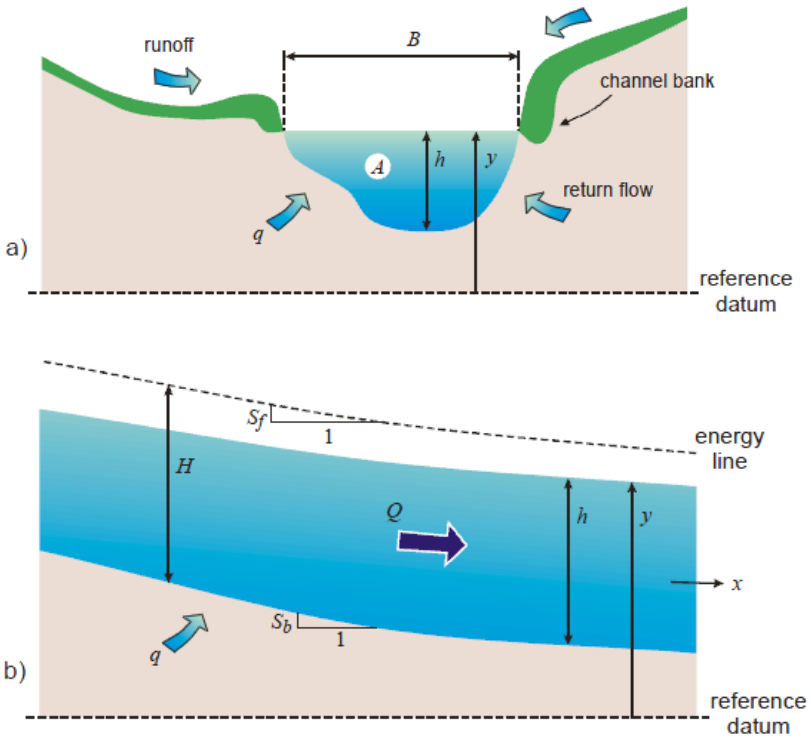

Figure 2-1. Visualization of variables used in the CONCEPTS hydraulics sub-model: (a) cross-sectional view and (b) longitudinal view (Langendoen, 2000), where *B* is flow top width, *A* is flow area, *h* is flow depth, *y* is referenced flow depth, *q* is lateral flow, S_b is bed slope, S_f is friction slope, *Q* is discharge, *x* is distance along the channel, and *H* is hydraulic head.

The sediment transport and streambed adjustment sub-model splits the channel into multiple layers, including a bed load layer and a wash load layer in the water column, and a surface layer and substrate layer in the streambed. For computational simplicity, the bed load and wash load are combined into a single, total load layer that exchanges sediment particles with the bed. The sediment flux between the water column and the bed are governed by the following mass balance equation:

$$\frac{\partial C_k}{\partial t} + \frac{\partial u C_k}{\partial x} = E_k - D_k + q_{sk} \tag{2.4}$$

$$C = \frac{1}{(1 \times 10^6)\frac{\gamma_s}{\gamma}} \int c \, dA \tag{2.5}$$

where t is time (s), x is distance along the channel centerline (m), u is the average flow velocity (m/s), E is the entrainment rate of particles from the bed (m^2/s), D is the deposition rate of particles onto the bed (m^2/s), q_s is the rate of sediment inflow from streambanks (m^2/s), the subscript k refers to the k^{th} particle size class, C is the sediment mass (m^2), c is a point concentration by weight (ppm), γ_s is the specific weight of sediment (N/m^3), and γ is the specific weight of water (N/m^3), and $1x10^6$ is an unit adjustment factor (Langendoen, 2000). Figure 2-2 shows a visualization of the variables used in the sediment transport and streambed adjustment sub-model. The entrainment and deposition rates, E and D, respectively, are calculated using different methods for cohesive and noncohesive bed materials. All of the bed materials used in this project are noncohesive, which use the Meyer-Peter Mueller transport equation (Langendoen, 2000).

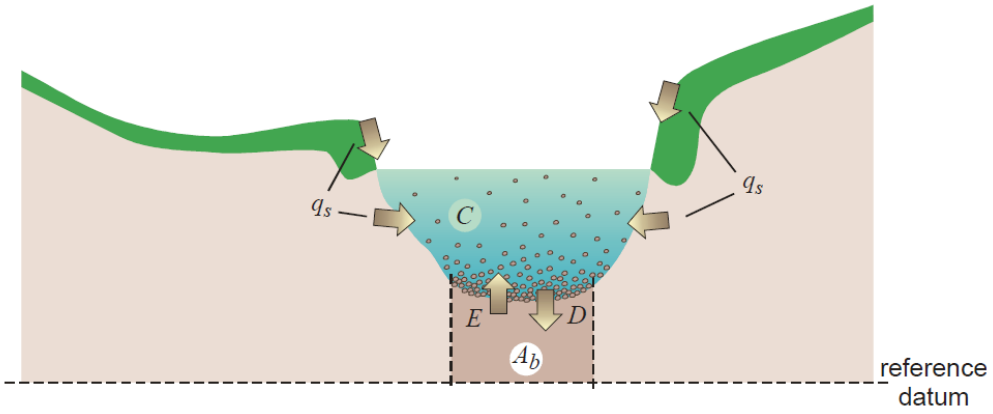

Figure 2-2. Visualization of variables used in the CONCEPTS sediment transport and streambed adjustment sub-model (Langendoen, 2000), where q_s is the rate of sediment inflow from streambanks and adjacent fields, C is sediment mass, E is entrainment rate, D is deposition rate, and A_b is cross sectional area of the mixing layer.

The bank erosion and stream width adjustment sub-model simulates the erosion processes occurring at each cross section. There are four main types of bank failure mechanisms, including rotational failures, planar failures, cantilever failures, and piping failures. However, at this time, CONCEPTS only simulates planar and cantilever failures. These mechanisms can be attributed to one of the two main processes simulated in CONCEPTS – fluvial erosion and mass wasting. Fluvial erosion is the entrainment of material particles on the bank face due to shear stresses caused by the hydraulic forces of the stream flow. Mass wasting encompasses the failure mechanisms outlined above and is a function of the resisting and driving forces within the streambank. Fluvial erosion may happen continuously over time while the mass wasting process is episodic.

CONCEPTS predicts erosion due to fluvial processes using the excess shear stress equation defined as:

$$\varepsilon = k_d(\tau - \tau_c) \tag{2.6}$$

where ε is the erosion or entrainment rate (m/s), k_d is an erodibility coefficient (m/s Pa), τ is the applied average shear stress (Pa), and τ_c is the critical shear stress (Pa) (Hanson and Cook, 2004). When the applied shear stress exceeds the critical shear stress, the bank face material actively erodes. The excess stress parameters, k_d and τ_c, can vary greatly based the soil properties of the bank face. In general, τ_c tends to be higher for cohesive soils compared to noncohesive soils and, therefore, erosion rates tend to be lower for cohesive soils compared to noncohesive soils (Langendoen, 2000).

Mass wasting, including planar and cantilever failures, is simulated in CONCEPTS using a *FS* approach that uses the ratio of the resisting forces divided by the driving forces within the streambank. The driving force is the gravitational force acting on the bank while the resistive force is the shear strength of the bank that includes frictional and cohesive forces. With a *FS* equal to one, the driving and resisting

forces are equal and a mass failure is probable (Simon et al., 2000). When *FS* is less than one, indicating that the driving force is larger than the resisting force, a bank failure occurs. When *FS* is greater than one, the bank is stable as the resisting forces are greater than the driving forces. The driving gravitational force in a streambank is given by

$$S_d = W sin\beta \tag{2.7}$$

where S_d is the driving force (Pa), W is the weight of the failure block (Pa), and β is the angle of the most critical failure plane. The primary force driving a mass failure is the weight of the block, which can be affected by factors such as fluvial erosion causing an increased bank height or slope angle, or by the moisture content of the soil that occurs with drawdown conditions leaving water in the top layer of the bank and draining water from the bottom layer. The resisting force can be expressed using a modified Mohr-Coulomb equation:

$$S_r = c' + \sigma \tan(\varphi') + \psi \tan\left(\varphi^b\right) \tag{2.8}$$

where S_r is the resisting force or shear strength (Pa), c' is the effective cohesion (Pa), σ is the net normal stress (Pa), ϕ' is the effective internal angle of friction (°), ψ is the matric suction (Pa), and ϕ^b is an angle that relates the shear strength and matric suction (°) (Simon et al., 2000).

2.4.2 RVR Meander Model

Although CONCEPTS is a robust, process-based model, like any model it has limitations and assumptions that must be taken into account. The most prominent of these is that CONCEPTS assumes a straight channel. The stream corridor is simulated in CONCEPTS as reaches connecting cross sections, or nodes, with information being exchanged forward and backward between the linear progressions of information nodes.

This assumption puts limitations on the realistic simulation of meandering rivers, particularly in terms of the bank erosion sub-model and the process of fluvial erosion.

Meander bends in rivers cause both curvature-driven and turbulence-driven secondary flows that alter the flow fields and the morphology of the bed and banks (Camporeale et al., 2007). River bends usually exhibit faster, deeper flow on the outside bend, and bank accretion and the formation of a point bar on the inside bend (Motta et al., 2012). These faster, deeper flows on the outside bend, along with the secondary flows, exert increased shear stresses on the streambank. Since CONCEPTS assumes a straight channel, these increased shear stresses are not being simulated.

For this project, the RVR Meander model was utilized to help overcome this issue with CONCEPTS. RVR Meander is a two-dimensional long-term meander migration model with a hydrodynamics and bed morphodynamics component, and a channel migration component (Motta et al., 2012). The first component characterizes the stream based on statistical analyses to calculate important components of stream shift and analyzes hydrodynamics and bed morphodynamics with respect to the channel centerline. The second component models the planform migration using a bank erosion sub-model based on increased near-bank velocities (Abad and Garcia, 2006). All calculations are made assuming bankfull flow and a constant channel depth and width.

2.4.3 Bank Stability and Toe Erosion Model

The Bank Stability and Toe Erosion Model (BSTEM) is the precursor to CONCEPTS that predicts annual streambank erosion at one site, and was developed by USDA-ARS. BSTEM is a Microsoft Excel based model that uses the *FS* approach to quantitatively assess the stability of existing and proposed channel banks using detailed input data. The model incorporates two primary processes, including bank failure by shearing and by flow of bank and bank toe material. It is capable of simulating different

streambank failure modes as well as the effects of streambank stabilization techniques that increase soil strength (Simon et al., 2001). These features make BSTEM a viable tool for estimating the risks of hydraulic erosion and bank failures. However, BSTEM only simulates one site at a time and is unable to account for upstream and downstream effects of bank erosion or bank stabilization.

The bank stability portion of BSTEM uses three limit equilibrium method models to calculate a *FS* for the streambank. These three models simulate horizontal layers, vertical slices with or without a tension crack, and cantilever shear failures. The horizontal layer method simulates saturated and unsaturated portions of the bank and incorporates up to five soil layers in the bank profile with different geotechnical properties. The vertical slice method is similar to the horizontal layer method with the addition of evaluating normal and shear forces active in segments of the failure area. Finally, the cantilever shear failure is a modification of the horizontal layer method where the failure plane angle is set equal to 90° to yield the *FS* estimation (Simon et al., 2001).

The toe erosion portion of the program calculates the average boundary shear stress, erodibility, critical shear stress, and the erosion rates and amounts. The bank stability model and the toe erosion model work together to predict an overall *FS* and a new failed or eroded bank profile.

As stated earlier, BSTEM can also incorporate bank stability methods to assess their effects on streambank erosion and factor of safety. BSTEM simulates mechanical effects of bank top vegetation using a root-reinforcement model that calculates an added soil cohesion factor. The other option is to simulate bank or bank-toe protection against hydraulic erosion by adding bank and toe protection treatments that increase the critical shear stress in the model.

While BSTEM looks at only one cross section at a time, CONCEPTS essentially “connects” multiple BSTEM cross sections and simulates reach processes. The

advantage of using CONCEPTS compared to BSTEM is the ability to evaluate upstream and downstream effects, which can be critical when identifying an optimal location for a streambank stabilization project.

CHAPTER III

METHODOLOGY

Application of CONCEPTS required a large amount of field data to be collected to parameterize the model. Data were collected from sites throughout the Illinois River basin in order to properly setup a physically accurate model.

3.1 Data Collection

Detailed stream reach data were collected at 37 sites within the Illinois River basin. Sites were distributed over a variety of stream orders in order to properly characterize the basin. Locations for data collection were chosen based on accessibility and bank stability. Data collection at each site included a cross-sectional survey, a bed pebble count, a Channel Stability Index, soil samples of the bed and the critical bank, site coordinates, digital photographs, and if applicable a bank pebble count, a jet erosion test (JET), and a borehole shear test (BST). A sample of the data collection packet used at each site is given in Appendix A. Cross-sectional surveys were completed using an automatic laser level (Spectra LL400), survey rod, and tape. Latitude and longitude site coordinates were taken to document site locations and digital photographs were taken for data verification and archiving.

Pebble counts for the beds and noncohesive banks were performed using the Wolman sampling method (Wolman, 1954), in which 100 random pebbles where sampled and measured along their intermediate axis. If the pebble counts contained more than 20% fines, a bulk soil sample was taken for additional laboratory analysis. For the cohesive bank materials, bulk soil samples were taken for lab analysis. The pebble counts and bulk samples were analyzed and used to provide particle size distributions and D_{50} measurements for all soil and sediment layers to be modeled.

A minimum of two JETs (Hanson et al., 1990) were performed *in situ* at each site where the streambanks had a cohesive soil layer. The JETs were conducted using a mini-jet and setup and operated following procedures outlined by Hanson and Cook (2004), Hanson and Hunt (2009) and Al-madhhachi et al. (2011). The purpose of the JETs was to measure the fluvial erosion parameters from Equation 2.6, k_d and τ_c, for the cohesive soils. The mini-jet works by shooting a small jet of water into the streambank at a constant pressure and measuring the amount of material eroded over time in the scour hole (Hanson and Robinson, 1990). The τ_c is estimated from these tests based on the equilibrium scour hole depth and k_d is estimated from the relationship between scour hole depth and the time to reach equilibrium.

A minimum of two BSTs were performed at sites that contained a cohesive soil layer to characterize the ability of the streambank soil to resist mass failures. Tests were conducted using procedures published by Handy Geotechnical Instruments, Inc. These tests measured the failure resistance parameters from Equation 2.8, c' and ϕ', for the cohesive soils at each site. The BST works by applying a shear and normal stress to the side walls of a borehole in the streambank. A shear head was inserted vertically into the borehole at a measured depth and a normal stress was applied. After the soil was allowed to consolidate, the shear head is pulled upward, applying a shear stress to the

soil in contact with the shear head. As seen in Equation 2.8, the matric suction of the soil during these tests had an effect on the calculated failure resistance parameters, so a soil sample was also taken from each of the boreholes. Each soil sample was analyzed with a tensiometer in the laboratory to measure soil moisture tension, and provided a soil cohesion adjustment due to water content. A second soil sample was also taken to measure the bulk density of the soil.

Finally, at each site a Channel Stability Index (CSI) was performed to qualitatively characterize the site (Simon and Downs, 1995). The CSI is a rapid assessment methodology that provides a numerical rank of bank stability based on nine components with a numerical score for each component. The nine components included primary bed material, bed or bank protection, estimated degree of incision, estimated degree of constriction, qualitative stream bank erosion due to fluvial processes or mass wasting, estimated percent of each bank failing, estimated riparian woody-vegetative cover, estimated fluvial deposition, and the stage of channel evolution according to the Channel Evolution Model (Simon and Rinaldi, 2006). Scores for each of the nine components were summed for a final CSI rank that provided a measure of the streambank stability at each site. Higher CSI scores indicated a more unstable streambank compared to lower CSI scores (Heeren et al., 2012).

3.2 Model Setup

Using these field data, a single 9.25 km reach was selected to be modeled in CONCEPTS based on data availability with multiple sites per reach, and the overall stability of the reach based on CSI results. Barren Fork Creek was selected due to the high number of sites visited and predominately unstable site conditions. A total of six sites in the reach were identified and included in the model (Table 3-1, Figure 3-1).

Table 3-1. Site locations on the Strahler fifth-order Barren Fork Creek reach in the Illinois River basin used in the CONCEPTS model.

Site Identifier	*Longitude*	*Latitude*
BF1	-94.83452	35.9229
BF2	-94.84752	35.9057
BF3	-94.85505	35.9027
BF4	-94.86507	35.8879
BF5	-94.87461	35.8837
BF6	-94.87805	35.8859

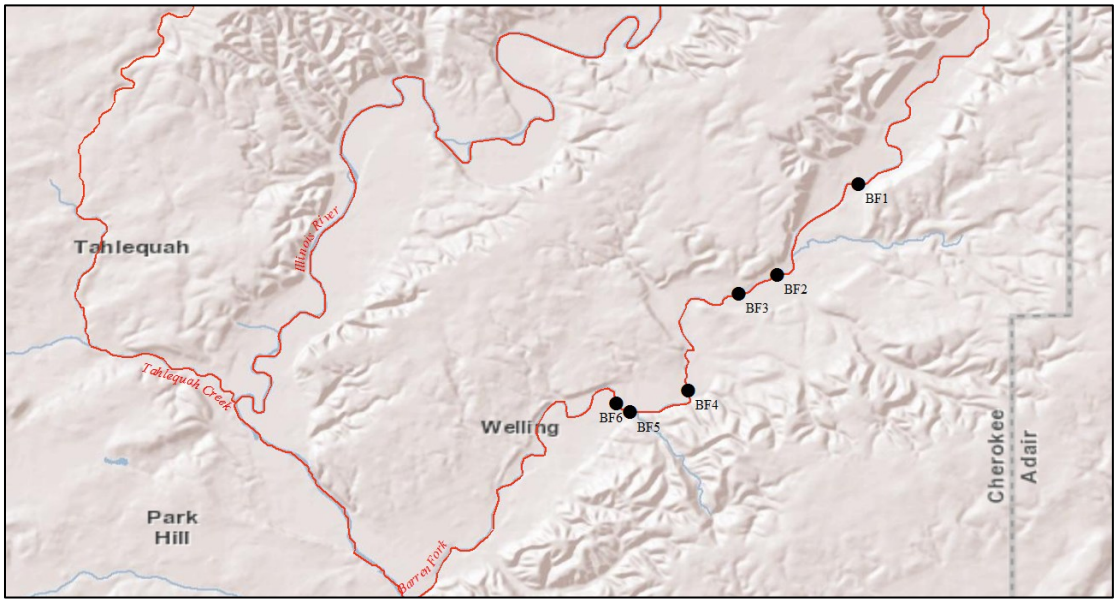

Figure 3-1. Site locations on the Strhaler fifth-order Barren Fork Creek reach in the Illinois River basin used in the CONCEPTS model.

A total reach length of 9.25 km was modeled in CONCEPTS from BF1 to BF6. Uniform spacing between sites was not possible due to accessibility issues through private property. Figure 3-2 shows the change in elevation over the 9.25 km reach and the slope between sites. There was an increased bed slope between sites BF4 and BF5, with all other slopes being comparable around 0.0007 m/m.

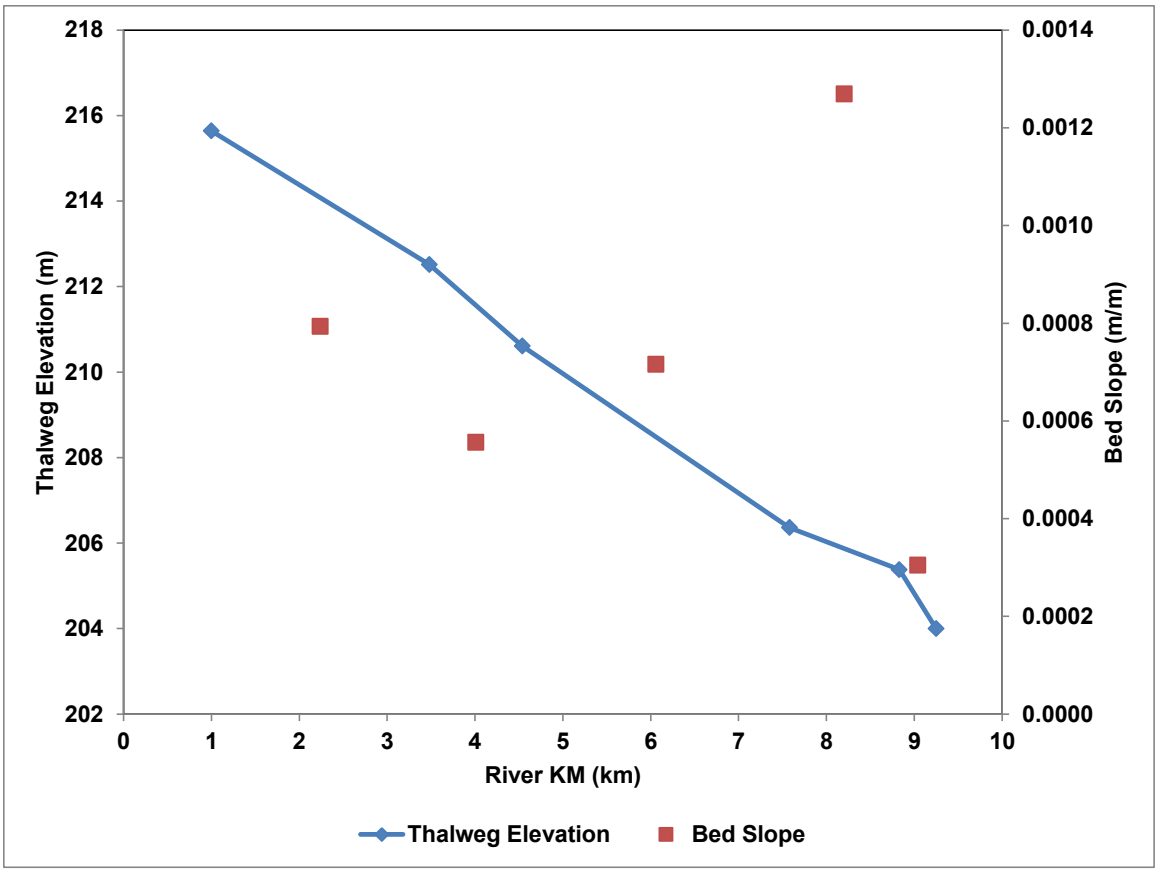

Figure 3-2. Thalweg elevation and bed slope between cross sections of the modeled reach including 6 cross sections located at 1.0, 3.5, 4.5, 7.6, 8.8, and 9.3 km.

Each site had a composite critical bank that usually contained a cohesive soil top layer and an unconsolidated gravel bottom layer and toe. All of the sites simulated were predominately unprotected by vegetation and had critical bank heights ranging from 1.0 to 9.5 m. Figures 3-3a, b, and c show a view of the critical bank, an aerial view, and a surveyed cross section at each site modeled.

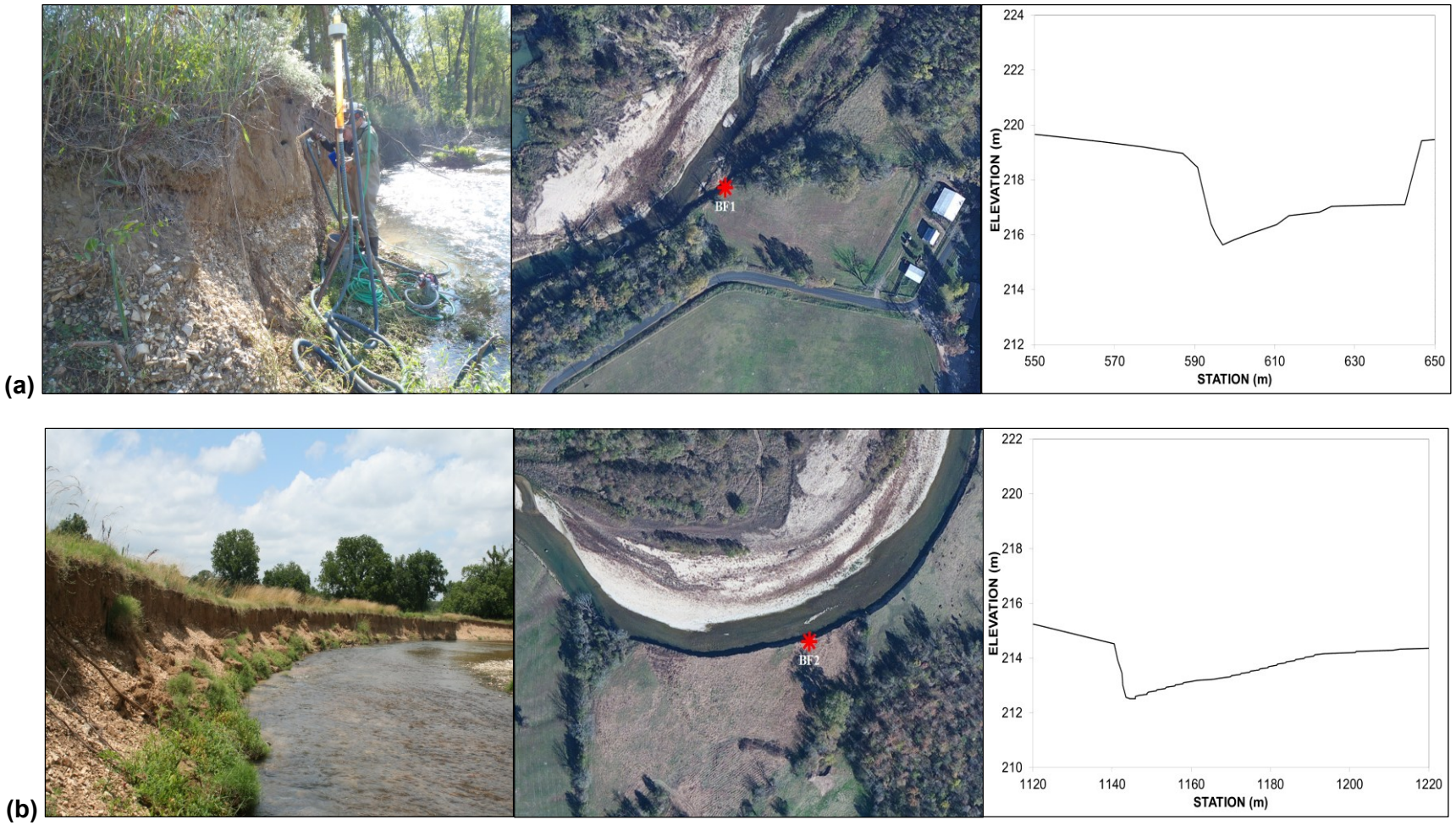

Figure 3-3a. Ground-based photograph, aerial imagery (USDA-FSA, 2010, 1:2000), and initial cross sectional survey at site (a) BF1 and (b) BF2.

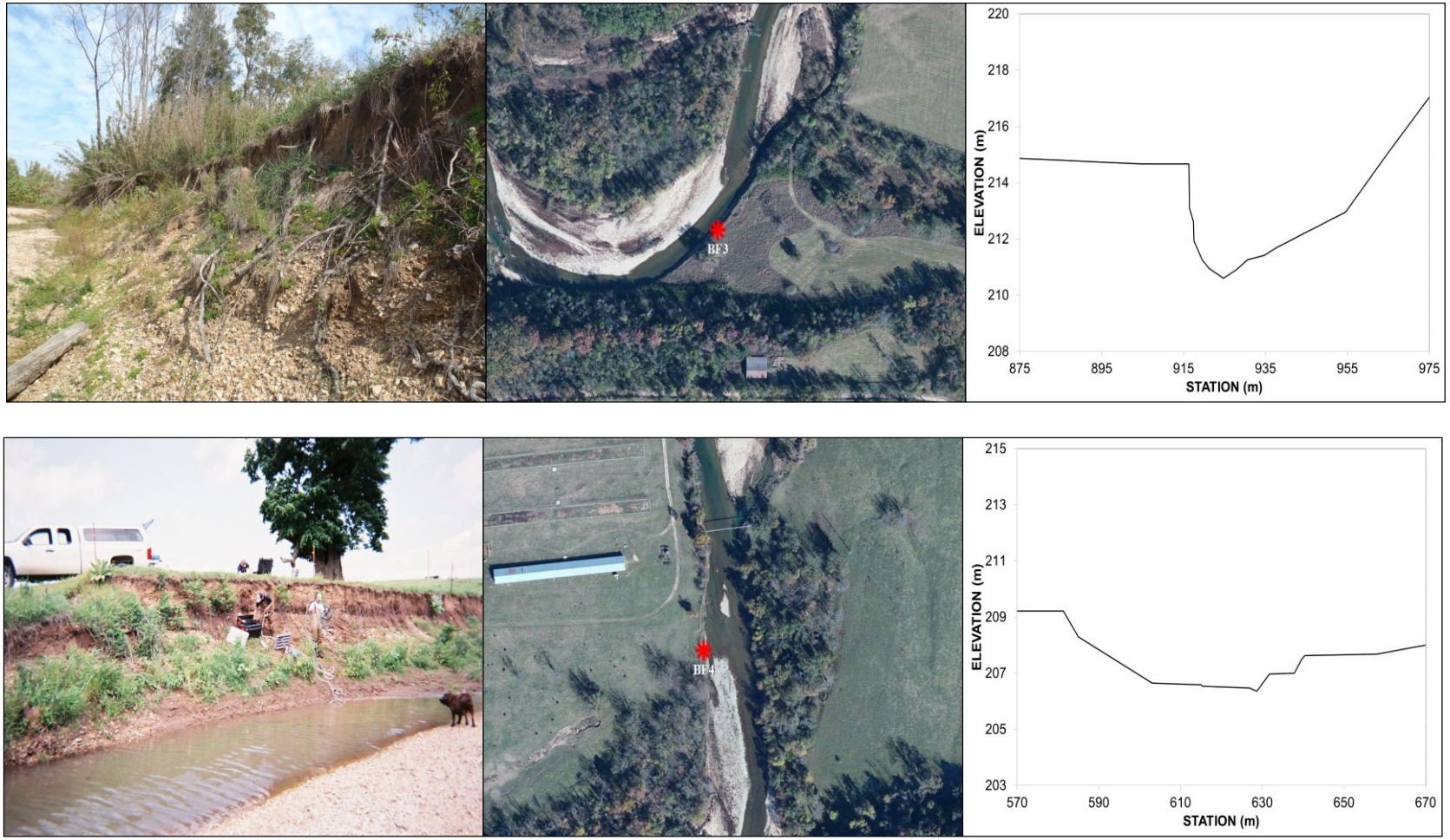

Figure 3-3b. Ground-based photograph, aerial imagery (USDA-FSA, 2010, 1:2000), and initial cross sectional survey at site (a) BF3 and (b) BF4.

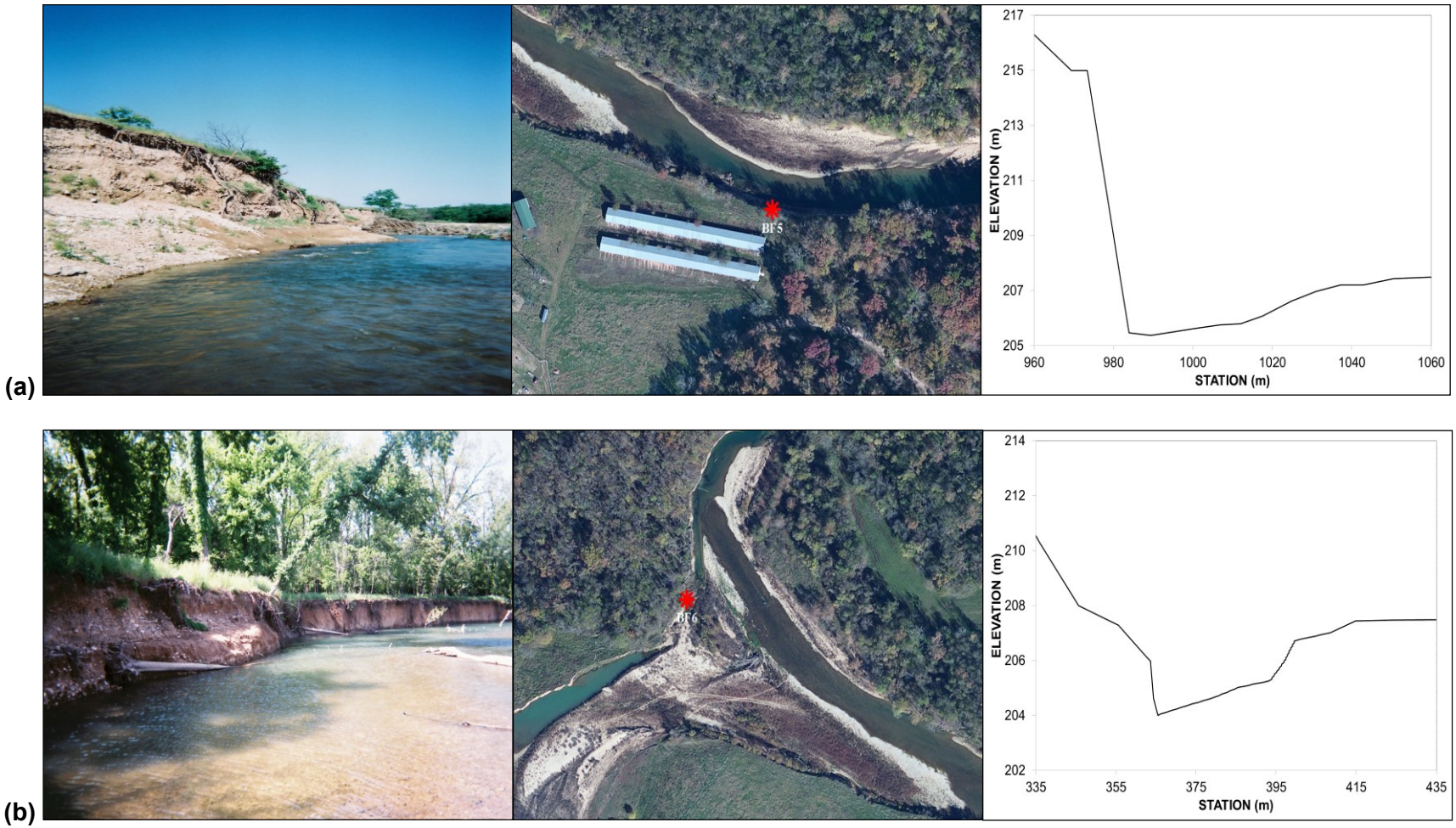

Figure 3-3c. Ground-based photograph, aerial imagery (USDA-FSA, 2010, 1:2000), and initial cross sectional survey at site (a) BF5 and (b) BF6.

The CONCEPTS model was built with a graphical user interface for data input, which was split into three main input sections: *Physical Data*, *Channel Models*, and *Run Data*. The *Physical Data* section included data for the sediments, soils, and cross sectional geometry for each cross section to be modeled. For the sediments and soils, the following input data were required: bulk density, particle density, porosity, permeability, critical shear stress, erodibility, cohesion, friction angle, suction angle, and a grain size distribution. Table 3-2 shows the origin of each input value used for the cohesive and noncohesive soils and sediments modeled. Appendix B includes all input data for each site (post-calibration). Note that the non-critical bank at each site was assigned the same properties as the bed material at each site.

For the cohesive soils, the bulk density was measured and analyzed from the core samples taken at each site, and the particle density was assumed to be 2650 kg/m^3 for all soils. Porosity was calculated based on the bulk and particle densities using the soil relationship shown in Table 3-2. The permeability of the cohesive soils was assumed to be 4x10^{-5} m/s based on previous infiltration experiments done at BF3 (Heeren et al., 2012). The critical shear stress and erodibility coefficient, and the cohesion and friction angle for each soil were calculated using site specific results from the JETs and BSTs, respectively. The suction angle was assumed to be 15° for all soils based on the default values reported in BSTEM (Simon et al., 2001).

For the noncohesive soils and bed sediments, the bulk density was assumed to be 2038.7 kg/m^3 based on the default values reported in BSTEM for gravel, and the particle density was assumed to be 2650 kg/m^3 for all soils. Porosity was calculated based on the bulk and particle densities.. The permeability of the noncohesive soils was assumed to be 2x10^{-3} m/s based on previous groundwater tracer studies done at BF3 (Fuchs et al., 2009). For all noncohesive soils and sediments, the critical shear stress

was estimated using the following algorithm developed for noncohesive gravel particles (Millar, 2005):

$$\tau_c = 0.048\tan(\varphi')\rho g(s-1)d_{50}\sqrt{1-\frac{\sin^2\theta}{\sin^2\varphi'}} \quad (3.1)$$

where ρ is the density of water (1000 kg/m^3), g is gravitational acceleration (9.81 m/s^2), s is the specific gravity of the bank soil (assumed to be 2.65 for all soils), d_{50} is the mean particle diameter of the soil (m), and θ is the bank angle (assumed to be 25° for all bank soils and 0° for all bed sediments). For the noncohesive soils a method to estimate the erodibility coefficient was not available, and therefore the erodibility coefficient was calibrated. The initial value for the erodibility coefficient was estimated using an inverse relationship between the critical shear stress and the erodibility coefficient developed for cohesive soils (Hanson and Simon, 2001):

$$k_d = 0.1 \times 10^{-6}\tau_c^{-0.5} \quad (3.2)$$

Next, k_d was adjusted via model calibration, with the calibration process discussed in the next section. For all noncohesive soils the cohesion was assumed to be zero and the angle of friction was assumed to be the angle of repose based on the mean particle diameter (Lane, 1955). Lastly, the suction angle was assumed to be 15° for all soils and sediments based on the default values reported in BSTEM.

The *Channel Models* input section included reaches, structures, tributary inflows, lateral inflows, and riparian buffers. For this study, only reaches were simulated. Only one reach was simulated and was comprised of six cross sections (Table 3-1).

Table 3-2. Origin of CONCEPTS input for the "Physical Data" component for cohesive and noncohesive soil parameters.

Parameter	*Cohesive Soils*	*Noncohesive Soils*
Bulk Density (ρ_b, kg/m^3)	Measured from samples	2040
Particle Density (ρ_p, kg/m^3)	2650	2650
Porosity (n)	$n = 1 - \frac{\rho_b}{\rho_p}$	$n = 1 - \frac{\rho_b}{\rho_p}$
Permeability (K, m/s)	4x10^{-5}	2x10^{-3}
Critical Shear Stress (τ_c, Pa)	Measured from JET	Algorithm
Erodibility (k_d, m/s-Pa)	Measured from JET	Algorithm
Cohesion (c', Pa)	Measured from BST	0
Friction Angle (ϕ', °)	Measured from BST	Angle of repose
Suction Angle (ϕ^b, °)	15	15

The *Run Data* section included options for how CONCEPTS models the selected reach. These options include the processes simulated, simulation times, inflow files, sediment transport options, and streambank erosion options. For all models, all processes were simulated including hydraulics, sediment transport, toe erosion, and bank stability. Sediment transport options and streambank erosion options were also kept constant for all models. Most notable from these options were that the wash load size class was set to be less than 0.063 mm and that positive pore-water pressures, matric suction, confining pressures, and groundwater table dynamics were all included.

This section also includes the upstream boundary condition inflow file. This file was created using data from USGS gage #07197000 that is located at the first site location, BF1, on the reach. All flow data approved for publication from this gage were

used to create an inflow file from October 1, 2007 to October 1, 2011 for a four year simulation (Figure 3-4).

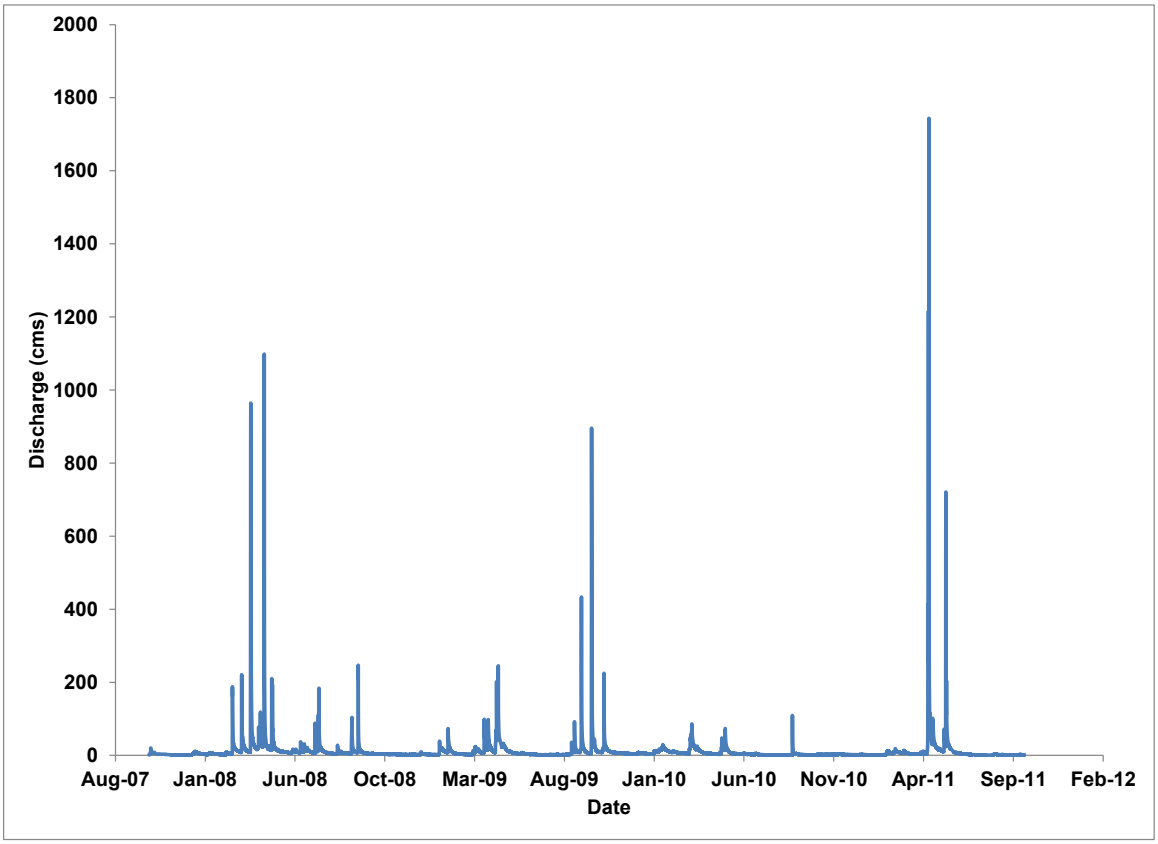

Figure 3-4. Hydrograph for four-year CONCEPTS simulation from 2007 to 2011 serving as the upstream boundary condition inflow file.

CHAPTER IV

EVALUTATION OF CONCEPTS

In order to build a realistic physical model, several steps were taken to calibrate and account for the limitations of CONCEPTS. CONCEPTS assumes a straight channel which significantly effects fluvial erosion when simulating a meandering stream; increased shear stresses on meander bends controlling erosion and transport of the bank materials is not simulated. Therefore, a correction factor must be estimated to properly simulate bank erosion and channel widening.

High uncertainty in many parameter estimates dictates the need for model calibration based on measured data. For example, a scientifically defendable method to estimate the erodibility coefficient for granular material was unavailable (Rinaldi et al., 2008).

4.1 Correcting for Channel Sinuosity

The first step towards developing a realistic model was estimating an adjustment factor, α, to account for the increased shear stress in the meander bends. Applied shear stress estimates at the bank for each site being modeled were calculated using the RVR

Meander model. RVR Meander was used to predict shear stress on the Barren Fork Creek near site BF3 is shown in Figure 4-1. These shear stresses are the average applied shear stress assuming constant channel width and depth at bankfull flow. Equation 2.6 defines fluvial erosion using a CONCEPTS predicted shear stress, *τ, with user defined* τ_c and k_d. The adjustment factor, *α*, was applied to the model using:

$$\varepsilon = k_d(\alpha\tau - \tau_c) = \alpha k_d\left(\tau - \frac{1}{\alpha}\tau_c\right) \tag{4.1}$$

Based on this equation, the erodibility coefficient had a direct relationship with *α* and the critical shear stress has an inverse relationship with alpha. Alpha was defined for each site as the ratio of the shear stress being applied at the bank site to the centerline applied shear stress (Langendoen and Simon, 2008; Rousselot, 2009; Langendoen and Simon, 2009). Table 4-1 shows the alpha values for all six sites. The RVR Meander output for all six sites included in the CONCEPTS model is given in Appendix C.

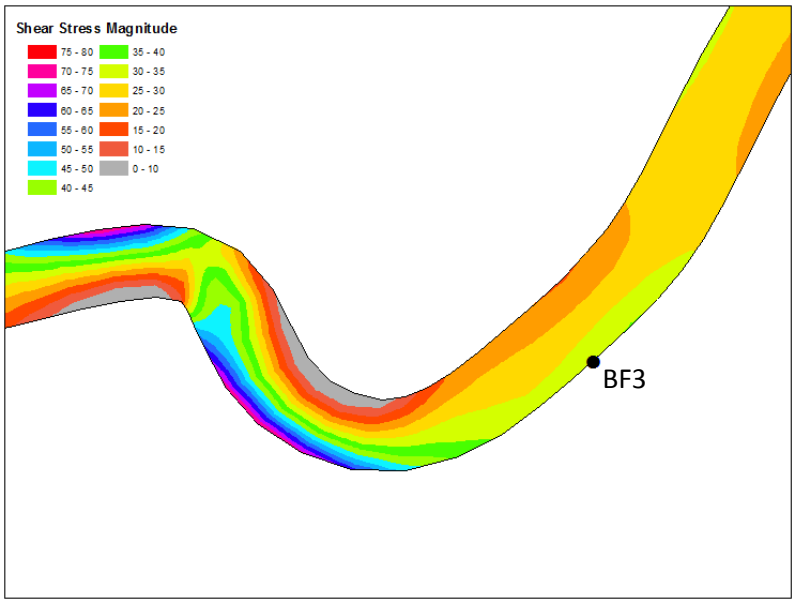

Figure 4-1. RVR Meander predicted magnitude of the applied shear stress (Pa) on the Barren Fork Creek near site BF3.

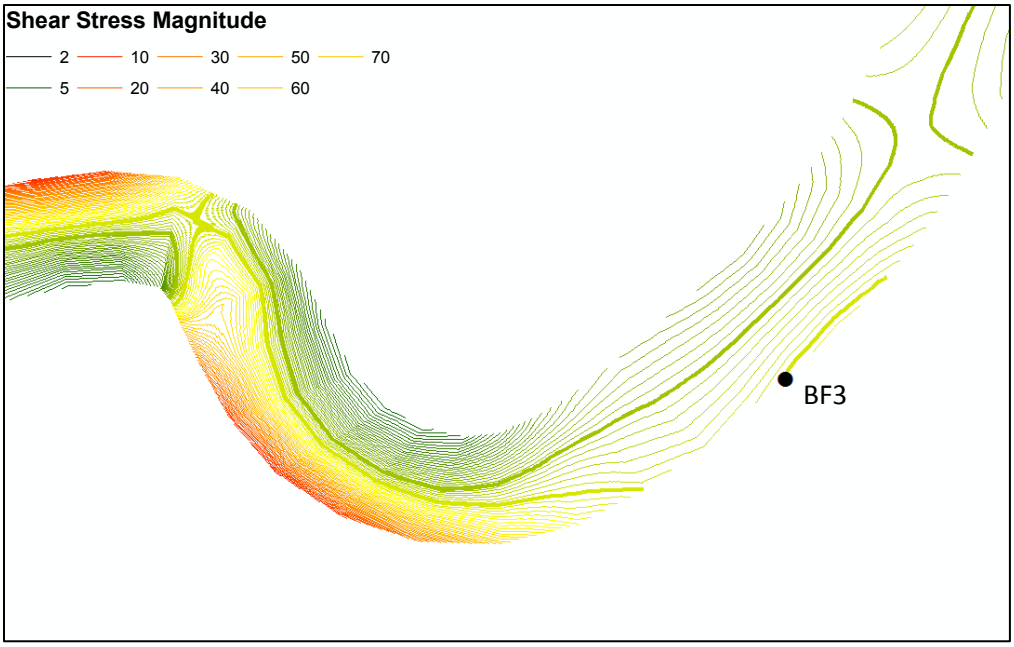

Figure 4-2. RVR Meander predicted magnitude of the applied shear stress (Pa) near site BF3 shown in one Pa contour intervals. The centerline and site BF3 near bank shear stresses are highlighted with bold lines.

Table 4-1. Barren Fork Creek alpha values used to correct for channel sinuosity for each site applied to the CONCEPTS model. The alpha factor was calculated as the ratio of the centerline applied shear stress to the bank applied shear stress.

Site	*Centerline Applied Shear Stress (Pa)*	*Bank Applied Shear Stress (Pa)*	*α*
BF1	27	27	1.00
BF2	27	51	1.89
BF3	27	34	1.26
BF4	27	29	1.07
BF5	27	42	1.56
BF6	27	51	1.89

These calculated alpha values were then applied to the fluvial erosion parameters, with alpha having a direct relationship with the erodibility coefficient and an

inverse relationship with the critical shear stress. Therefore, sites with a higher alpha value will simulate increased fluvial erosion due to the increased stresses within the bends. The measured or calculated fluvial erosion parameter values at each site, and the resulting parameters with the application of the alpha correcting factor, or the "modified" parameters are given in Table 4-2. These modified parameters were the parameters used as input into the model calibration.

Ideally, α would be included within the framework of CONCEPTS and would change with flow conditions. The α factor used in this study is for bankfull flow and a constant channel width and depth. With higher flows, α may increase with increased applied shear stresses, and vice versa with lower flows. Therefore, the α factors used in this study may be overestimating fluvial erosion when the flow is below bankfull and underestimating the fluvial erosion when the flow is above bankfull. These limitations and concerns are discussed later.

Table 4-2. Modified fluvial erosion parameters including the calculated alpha factor. The critical shear stress is inversely related to alpha and the erodibility is directly related to alpha.

Site	*Soil Type*	*α*	*τ_c (Pa)*	*Modified τ_c (Pa)*	*k_d (m/s Pa)*	*Modified k_d (m/s Pa)*
BF1	Cohesive	1.00	0.077	0.077	5.87E-09	5.87E-09
BF1	Noncohesive	1.00	5.482	5.482	4.27E-08	4.27E-08
BF2	Cohesive	1.89	0.176	0.093	1.68E-05	3.17E-05
BF2	Noncohesive	1.89	4.239	2.244	4.86E-08	9.17E-08
BF3	Cohesive	1.26	0.133	0.106	5.00E-06	6.30E-06
BF3	Noncohesive	1.26	12.224	9.707	2.86E-08	3.60E-08
BF4	Cohesive	1.07	0.341	0.317	1.73E-05	1.86E-05
BF4	Noncohesive	1.07	9.004	8.383	3.33E-08	3.58E-08
BF5	Noncohesive	1.56	9.312	5.986	3.28E-08	5.10E-08
BF6	Cohesive	1.89	0.130	0.069	2.77E-06	5.23E-06
BF6	Noncohesive	1.89	6.814	3.607	3.83E-08	7.24E-08

4.2 Sensitivity Analysis

After adjusting for channel sinuosity, a model calibration was required to develop a realistic CONCEPTS model. To aid in the calibration process a sensitivity analysis was first performed to identify the most sensitive parameters. A semi-local approach was used in which most input parameters were varied one at a time while all other parameters were held constant at their measured or assumed values. The input parameters selected for the sensitivity analysis were α, τ_c, k_d, c', φ', and K. These parameters were chosen because of their direct effects on bank erosion through both fluvial and geotechnical mechanisms. Model output parameters investigated included the total sediment yields of fines, sands, and gravels, the change in bed elevation, and the lateral retreat at the toe elevation. A relative sensitivity coefficient, S_r, was used and defined as:

$$S_r = \frac{P}{O}\left(\frac{O_2 - O_1}{P_2 - P_1}\right) \tag{4.2}$$

where P is the baseline parameter and O is the baseline predicted model output, P_1 and P_2 are input parameters varied plus and minus by a fixed interval from the baseline, and O_1 and O_2 are their corresponding output values (Haan et al., 1995; White and Chaubey, 2005). This relative sensitivity coefficient is dimensionless and provides information on the change in the model output for a given change in a model input parameter. The higher the sensitivity ratio, the more sensitive the model output is to the specific input parameter. While this provides guidance on which input parameters to focus on during model calibration, the results should be used with caution. This technique assumes a linear relationship model response and does not consider the interactions between parameters (White and Chaubey, 2005). For a natural channel system this can be

especially problematic due to the complexity of parameter interactions; however for the purposes of this study this technique provides reasonable guidance.

Each input parameter was varied differently in order to stay within their physical constraints and based upon expected values of the parameter. Table 4-3 shows each parameter and their range used in the sensitivity analysis. The baseline values were measured or calculated and are labeled here zero for no change. For all input parameters, if the low value became negative it was simulated at zero. As stated, a local approach was used with the following exceptions: changes in α also changed τ_c and k_d and changes in φ' also changed the noncohesive τ_c.

Table 4-3. Selected input parameters and their range (high and low) used in the sensitivity analysis. The zero values stand for no change to the measured parameter while the other values indicate the amount of change applied to the parameter.

Parameter	*Layer*	*Low[a]*	*Base*	*High*
α (Pa/Pa)	Cohesive	-0.25	0	+0.25
	Noncohesive	-0.25	0	+0.25
τ_c (Pa)	Cohesive	-50%	0	+50%
	Noncohesive	-50%	0	+50%
k_d (m/s-Pa)	Cohesive	-1×10^{-2}	0	$+1 \times 10^{-2}$
	Noncohesive[b]	1×10^{-6}	$1E^{-3}$	1
c' (Pa)[c]	Cohesive	0	+500 Pa	+1000 Pa
	Noncohesive	0	+300 Pa	+750 Pa
φ' (°)	Cohesive	-25%	0	+25%
	Noncohesive	-25%[d]	0	+25%
K (m/s)	Cohesive	-25%	0	+25%
	Noncohesive	-25%	0	+25%

[a] Parameters that became negative were simulated at a value of zero.
[b] There was no measured or calculated value for the noncohesive erodibility coefficient; thus a subjective range was used.
[c] Due to the measured value of zero, c' was increased by two interval steps.
[d] Based on the Millar (2005) algorithm used to calculate τ_c, φ' must be greater than or equal to the assumed bank angle of 25°. Any angles that became less than 25° were simulated at 25°.

The sensitivity analysis was performed by varying one input parameter at a time for all soil layers on the critical bank at each site. All other input parameters were kept constant, including the bed materials and the non-critical bank materials. The simulation was performed for a one month period for May 2009, which was short enough to accommodate a large number of simulations while still simulating a variety of flow events. Figure 4-3 shows the hydrograph for May 2009 from US Geological Survey gage number 07197000 used for the analysis. Approximately five storm events were included in the analysis varying from 30 to 250 m^3/s.

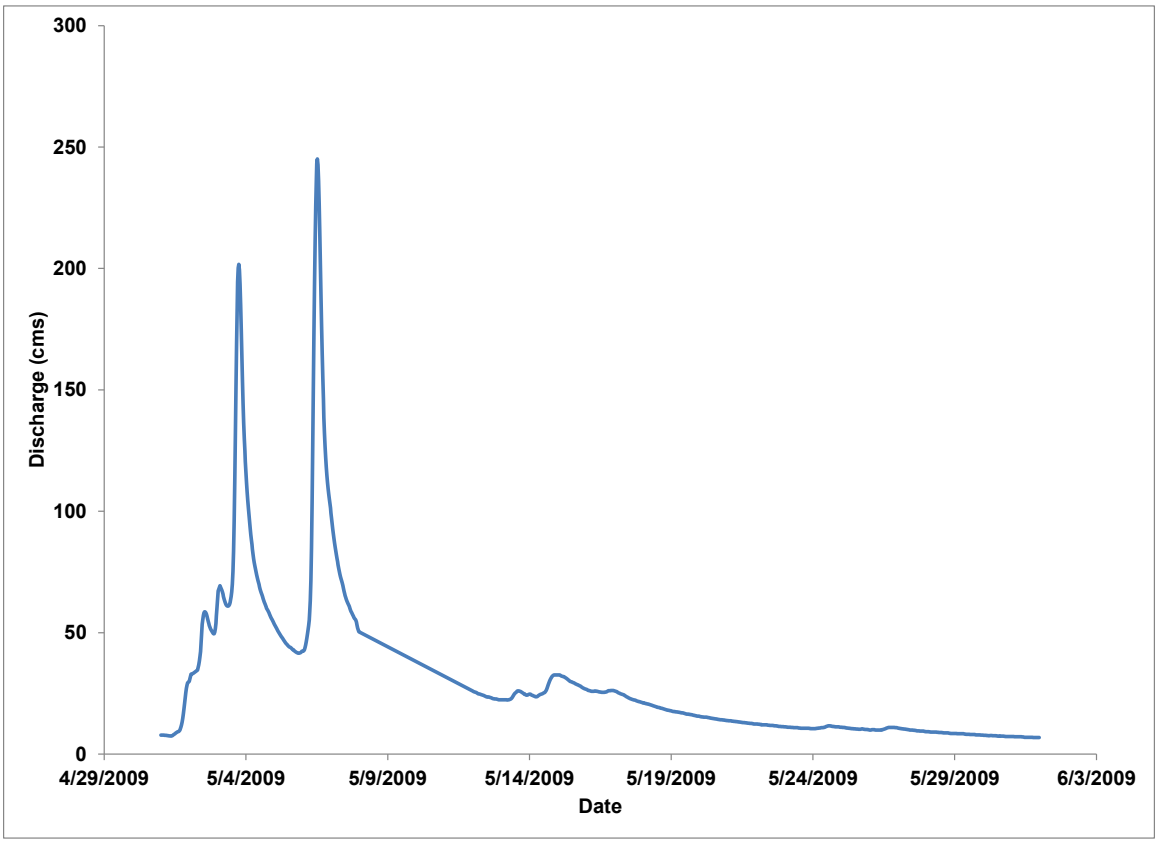

Figure 4-3. Barren Fork Creek hydrograph for May 2009 used to conduct the sensitivity analysis; US Geological Survey gage number 07197000.

The sensitivity analysis results (Table 4-4) showed little variation between cohesive and noncohesive soils but high variation between sites. This may be due, in part, to the individual make-up of each site, including bank materials, layering, and cross section. Another possible reason may result from additional parameters, such as the assumed bank angle or the suction angle, or processes, such as the simulated groundwater lag, that were not considered in the analysis which could have significant effects on bank failures. Also, many of the higher relative sensitivity coefficients occurred at BF1 and BF6, and thus they may be an artifact of a boundary issue within the model code occurring at the beginning and the end of the model reach.

Table 4-4. Relative sensitivity coefficients for sensitivity analysis.

α Sr										
Site	**Fines (tonnes)**		**Sands (tonnes)**		**Gravels (tonnes)**		**Lateral Erosion (m)**		**Bed Change (m)**	
	Cohesive	***Noncohesive***	***Cohesive***	***Noncohesive***	***Cohesive***	***Noncohesive***	***Cohesive***	***Noncohesive***	***Cohesive***	***Noncohesive***
BF1	3.76	3.76	0.11	0.11	0.43	0.43	1.44	1.44	3.00	3.00
BF2	1.24	1.24	1.81	1.81	*	*	0.51	0.51	0.91	0.91
BF3	0.66	0.66	0.51	0.51	0.19	0.19	1.23	1.23	1.20	1.20
BF4	0.35	0.35	0.69	0.69	2.25	2.25	0.21	0.21	0.37	0.37
BF5	**	0.26	**	0.27	**	2.99	**	2.35	**	0.68
BF6	0.29	0.29	0.58	0.58	18.5	18.5	47.8	47.8	11.3	11.3
Mean	1.26	1.09	0.74	0.66	5.35	4.88	10.23	8.91	3.36	2.92
Median	0.66	0.50	0.58	0.55	1.34	2.25	1.23	1.33	1.20	1.05

τ_c *Sr*										
Site	**Fines (tonnes)**		**Sands (tonnes)**		**Gravels (tonnes)**		**Lateral Erosion (m)**		**Bed Change (m)**	
	Cohesive	***Noncohesive***	***Cohesive***	***Noncohesive***	***Cohesive***	***Noncohesive***	***Cohesive***	***Noncohesive***	***Cohesive***	***Noncohesive***
BF1	1.46	1.46	0.09	0.09	0.16	0.16	0.85	0.85	1.75	1.75
BF2	1.18	1.18	0.11	0.11	*	*	1.29	1.29	0.71	0.71
BF3	1.00	1.00	0.40	0.40	0.10	0.10	1.12	1.12	0.52	0.52
BF4	0.12	0.12	0.10	0.10	0.46	0.46	0.36	0.36	0.32	0.32
BF5	**	0.18	**	1.30	**	39.1	**	0.93	**	0.37
BF6	0.15	0.15	0.42	0.42	5.12	5.12	28.0	28.0	5.00	5.00
Mean	0.78	0.68	0.22	0.40	1.46	8.98	6.33	5.43	1.66	1.45
Median	1.00	0.59	0.11	0.25	0.31	0.46	1.12	1.02	0.71	0.62

k_d Sr										
Site	**Fines (tonnes)**		**Sands (tonnes)**		**Gravels (tonnes)**		**Lateral Erosion (m)**		**Bed Change (m)**	
	Cohesive	***Noncohesive***	***Cohesive***	***Noncohesive***	***Cohesive***	***Noncohesive***	***Cohesive***	***Noncohesive***	***Cohesive***	***Noncohesive***
BF1	0.02	2E-05	2E-03	2E-06	1E-03	1E-06	0.01	1E-05	0.02	2E-05
BF2	0.71	7E-04	0.01	9E-06	*	*	0.02	2E-05	0.01	1E-05
BF3	0.41	4E-04	0.01	9E-06	7E-04	7E-07	0.01	7E-06	5E-03	5E-06
BF4	0.11	1E-04	0.00	1E-06	0.10	1E-04	0.02	2E-05	0.01	1E-05
BF5	**	7E-05	**	2E-05	**	4E-05	**	2E-05	**	2E-05
BF6	0.02	2E-05	0.01	1E-05	0.15	1E-04	0.22	2E-04	0.23	2E-04
Mean	0.26	2E-04	0.01	8E-06	0.06	6E-05	0.05	5E-05	0.05	5E-05
Median	0.11	9E-05	0.01	9E-06	0.05	4E-05	0.02	2E-05	0.01	2E-05

c' Sr										
Site	**Fines (tonnes)**		**Sands (tonnes)**		**Gravels (tonnes)**		**Lateral Erosion (m)**		**Bed Change (m)**	
	Cohesive	***Noncohesive***	***Cohesive***	***Noncohesive***	***Cohesive***	***Noncohesive***	***Cohesive***	***Noncohesive***	***Cohesive***	***Noncohesive***
BF1	0.81	0.81	0.01	0.01	0.02	0.02	0.58	0.58	0.50	0.50
BF2	3.13	0.87	0.08	0.02	*	*	0.86	0.24	0.27	0.07
BF3	9.02	0.85	2.19	0.21	0.33	0.03	5.82	0.55	2.28	0.21
BF4	0.32	0.32	0.01	0.01	0.12	0.12	0.01	0.01	0.02	0.02
BF5	**	0.27	**	0.09	**	*	**	0.01	**	0.00
BF6	0.14	0.14	0.30	0.30	0.21	0.21	0.08	0.08	0.00	0.00
Mean	2.68	0.54	0.52	0.11	0.17	0.10	1.47	0.24	0.62	0.14
Median	0.81	0.57	0.08	0.06	0.17	0.08	0.58	0.16	0.27	0.05

φ' Sr										
Site	**Fines (tonnes)**		**Sands (tonnes)**		**Gravels (tonnes)**		**Lateral Erosion (m)**		**Bed Change (m)**	
	Cohesive	***Noncohesive***	***Cohesive***	***Noncohesive***	***Cohesive***	***Noncohesive***	***Cohesive***	***Noncohesive***	***Cohesive***	***Noncohesive***
BF1	15,100.	15,500.	3.87	3.97	1.78	1.83	6.80	6.97	313.	321.
BF2	171.	187.	1.71	1.87	*	*	8.49	9.25	3.75	4.08
BF3	72.50	72.50	1.02	1.02	0.23	0.23	8.32	8.32	14.7	14.7
BF4	1.57	1.57	0.21	0.21	0.30	0.30	0.02	0.02	0.07	0.07
BF5	**	1.08	**	0.00	**	6.81	**	1.57	**	0.44
BF6	5.55	5.55	2.45	2.45	573	573.	174.	174.	33.3	33.3
Mean	3080.	2630.	1.85	1.59	144.	116.	39.5	33.3	73.0	62.2
Median	72.50	39.02	1.71	1.44	1.04	1.83	8.32	7.65	14.7	9.37

K Sr										
Site	**Fines (tonnes)**		**Sands (tonnes)**		**Gravels (tonnes)**		**Lateral Erosion (m)**		**Bed Change (m)**	
	Cohesive	***Noncohesive***	***Cohesive***	***Noncohesive***	***Cohesive***	***Noncohesive***	***Cohesive***	***Noncohesive***	***Cohesive***	***Noncohesive***
BF1	0.09	0.09	0.03	0.03	0.05	0.05	0.01	0.01	0.50	0.50
BF2	0.05	0.05	0.12	0.12	*	*	0.07	0.07	0.03	0.03
BF3	0.00	0.00	0.13	0.13	0.14	0.14	0.56	0.56	0.67	0.67
BF4	0.01	0.01	0.01	0.01	0.24	0.24	0.00	0.00	0.07	0.05
BF5	**	0.00	**	0.01	**	0.00	**	0.02	**	0.00
BF6	0.01	0.01	0.03	0.03	0.29	0.29	0.24	0.24	0.00	0.00
Mean	0.03	0.03	0.06	0.05	0.18	0.14	0.18	0.15	0.25	0.21
Median	0.01	0.01	0.03	0.03	0.19	0.14	0.07	0.04	0.07	0.05

* Sr cannot be calculated due to an output value of zero.
** Site BF5 did not have a cohesive layer.

Figures 4-4a and b show box plots for each of the input parameters and their relative sensitivity coefficients with the selected output parameters for cohesive and noncohesive layers separately. The boxplots suggest that φ' is the most sensitive input parameter for all output parameters for both cohesive and noncohesive soils. Also, k_d, appears to be the least sensitive for all output parameters for both cohesive and noncohesive soils with K also being the least sensitive for the cohesive soils.

The distributions for median values from the six sites (Figure 4-5) show that φ' is generally the most sensitive relative sensitivity coefficient followed by α, τ_c, c', and finally K and k_d for both cohesive and noncohesive soils. By understanding the sensitivity of input parameters on the model output, a priority scheme for the model calibration may be developed.

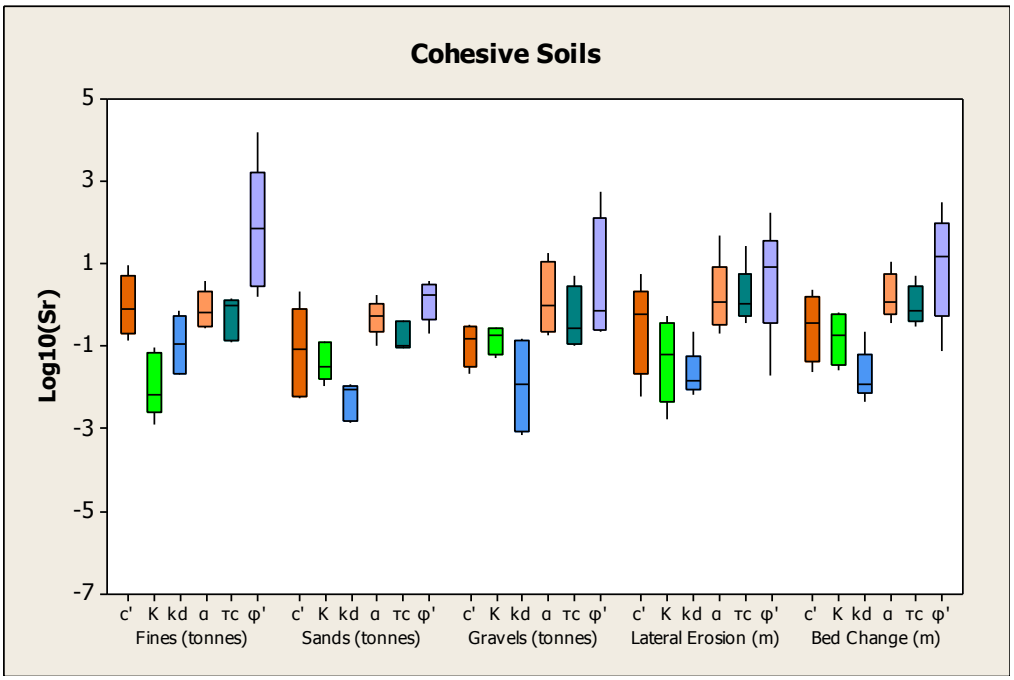

Figure 4-4a. Boxplots of relative sensitivity coefficients (S_r) for cohesive soils. Input parameters included c', k_d, α, τ_c, φ', and K. Output parameters included yields of fines, sands, and gravels, lateral erosion, and bed elevation change.

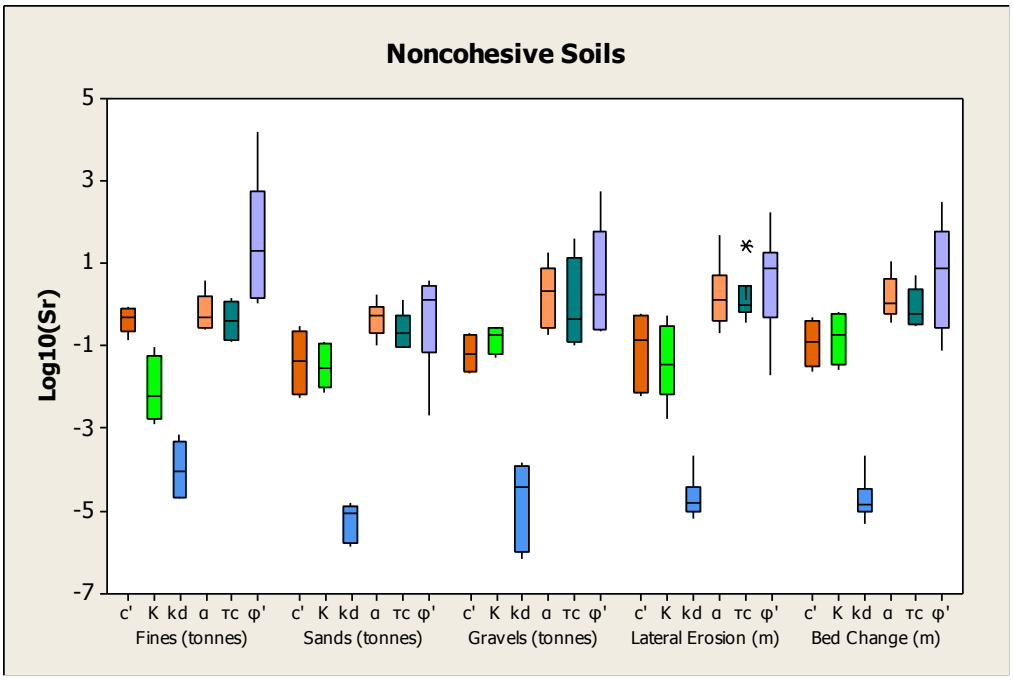

Figure 4-4b. Boxplots of relative sensitivity coefficients (S_r) for noncohesive soils. Input parameters included *c'*, k_d, α, τ_c, φ', and *K*. Output parameters included yields of fines, sands, and gravels, lateral erosion, and bed elevation change.

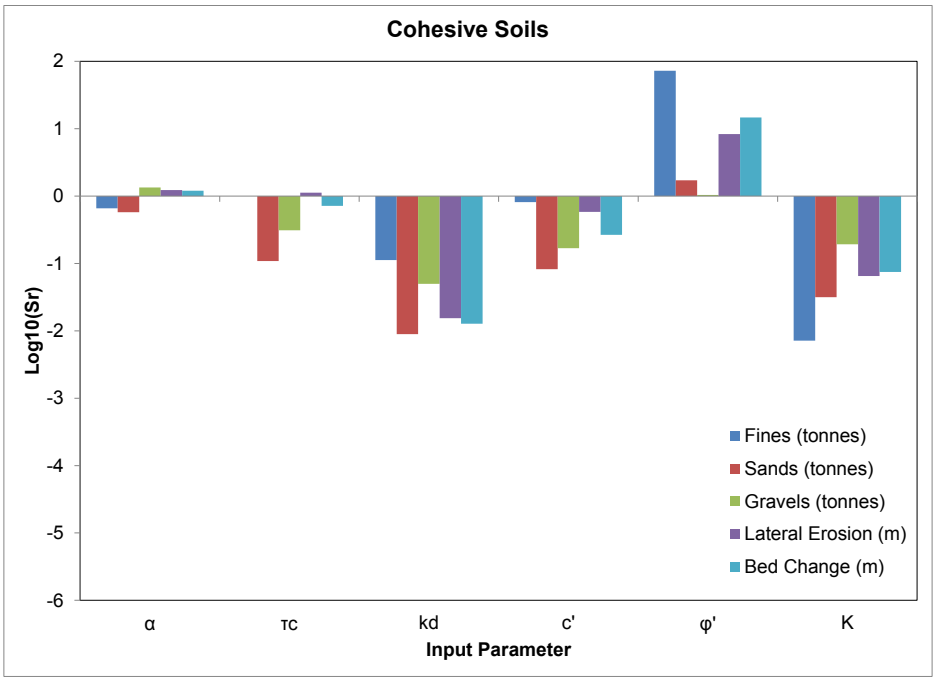

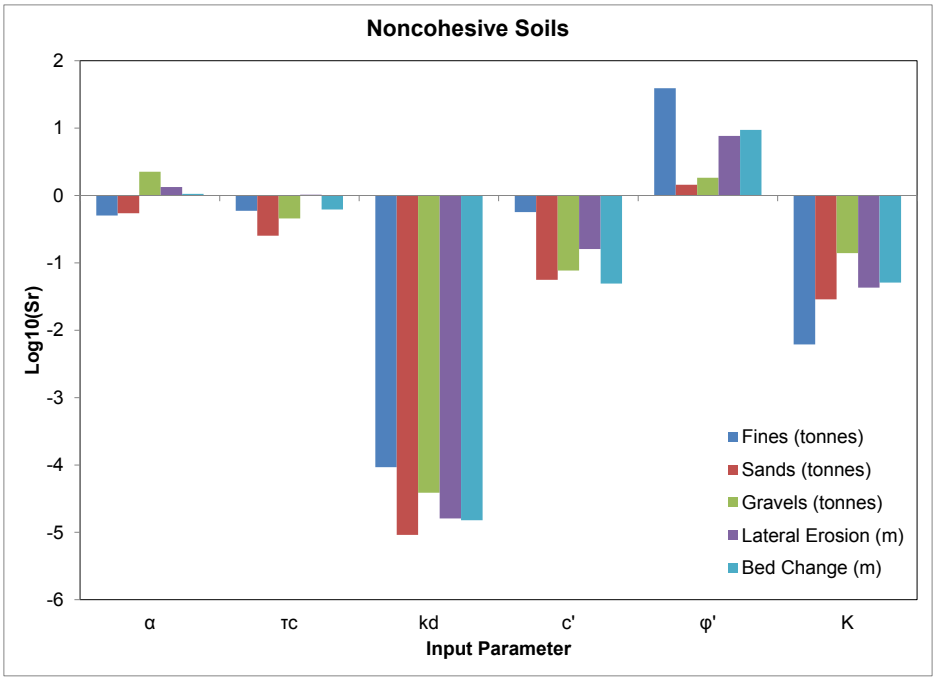

Figure 4-5. Median relative sensitivity coefficients for cohesive and noncohesive soils. Input parameters included *c'*, k_d, *α*, τ_c, *φ'*, and *K*. Output parameters included yields of fines, sands, and gravels, lateral erosion, and bed elevation change.

Although φ' and α were the most sensitive, the parameter used for model calibration was the critical shear stress, τ_c. Since φ' is a function of the mean particle size, which is a property of the bank material, and was based on measured data with a high degree of confidence, φ' was not altered. Also, α was not altered since it was calculated based on the RVR Meander outputs, which provided a reasonable estimate of the shear stress distribution throughout the reach. For c', it was either measured *in situ* for the cohesive soil layers or estimated to be zero for the noncohesive layers. While the estimates for the effective cohesion of the noncohesive layer had high uncertainty, there was no alternative method or measurement. Thus, c' was left at its measured or estimated value and not altered. For K, input parameters were based on previous measured data so it was likewise not altered. The two remaining parameters with a large degree of uncertainty were τ_c and k_d. Because τ_c had a much higher relative sensitivity than k_d, τ_c was chosen as the calibration parameter.

Not only did τ_c have a high relative sensitivity, but assumptions used to estimate the noncohesive τ_c could potentially be corrected with model calibration. The noncohesive τ_c was estimated using Equation 3.1 and thus the θ estimate becomes critical. The stability of the bank in terms of τ_c decreases with an increasing θ (Millar, 2005). Many, if not all, of the banks on the study reach exhibit near vertical profiles; however Equation 3.1 also constrains φ' to be greater than the bank angle. Therefore, the internal angle of friction, φ', was calculated based on the mean particle size and the bank angle, θ, was then assumed to be 25° in order to accommodate all friction angles. Millar (2000) suggests that φ' may encompass more than just the angle of repose for gravel layers, and recommends φ' represents a lumped parameter accounting for processes such as the influence of vegetation, and packing and cementing due to interstitial fines. By altering τ_c in the calibration process, θ and φ' estimates were

indirectly calibrated. Since τ_c of the cohesive layers was measured *in situ*, the calibration focused on the noncohesive τ_c that were dependent on θ and φ'.

4.3 Model Calibration

The site chosen for model calibration was BF3 since it had documented bank retreat and was the focus of multiple research projects that provided additional data and observations (Fuchs et al., 2009; Midgely et al., 2012; Heeren et al., 2012). BF3 had a 3.5 m critical bank with the top 1.3 m being cohesive silt and the bottom 2.2 m being a noncohesive gravel layer. The length of the streambank investigated was 100 m long. Two data sets were available for calibration at BF3 that measured lateral retreat of the critical bank over time. First, ground based data were available over a six month period from April to October 2009. There were a series of storms (Figure 4-6) during this time period, two of which were greater than 400 m^3/s and caused significant erosion and lateral streambank migration.

Ground based measurements estimated an approximate critical bank retreat of 8 to 22 m, depending on the bank location, and an average of 15 m from measured bank profiles between April 18, 2009 and October 12, 2009 (Midgley et al., 2012). These ground-based data consisted of four measurements on April 18, May 15, September 26, and October 12, 2009.

The second data set available for calibration at BF3 was May 4, 2008 and August 9, 2010 NAIP aerial imagery (USDA-FSA, 2008 and 2010). Between 2008 and 2010 aerial imagery estimated critical bank retreat was approximately 10 to 30 m, depending on the bank location, with an average of 20 m (Figure 4-7).

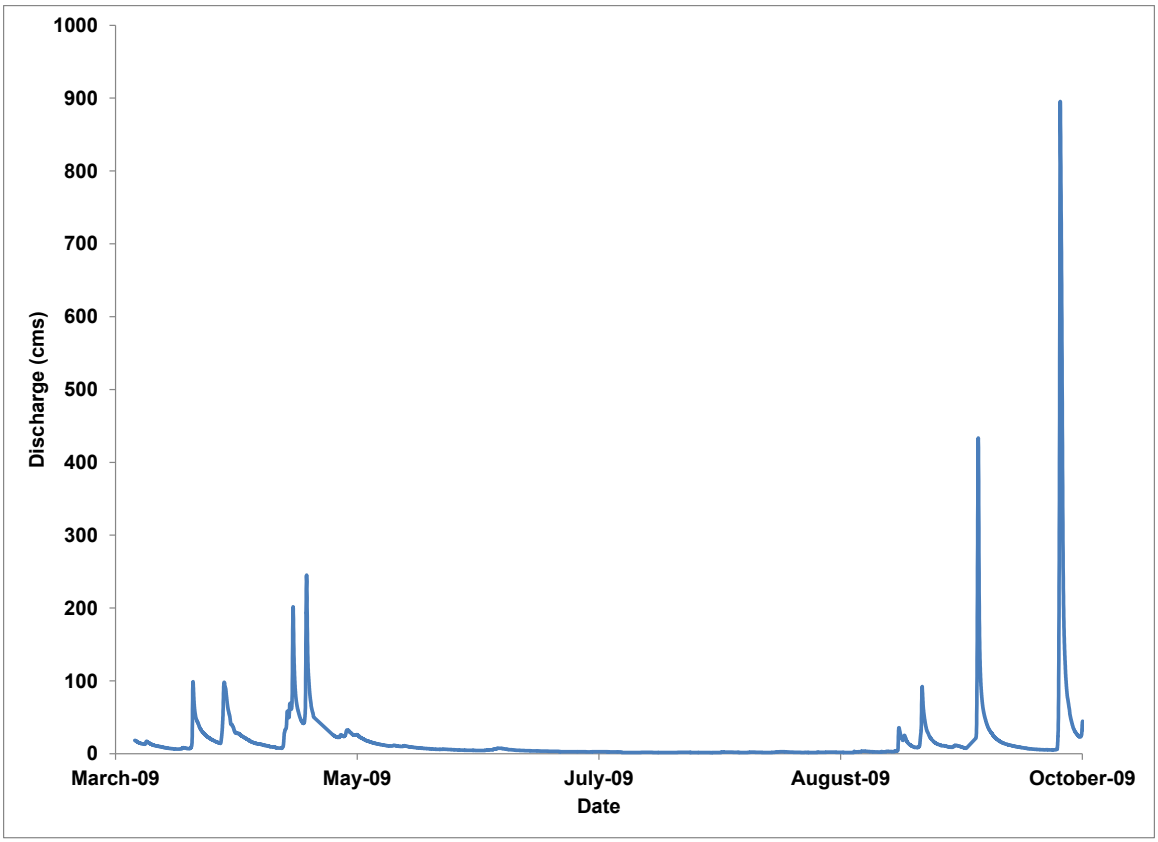

Figure 4-6. US Geological Survey Barren Fork Creek gage number 07197000 hydrograph from April to October 2009 applicable to ground based data used in model calibration.

Figure 4-7. Lateral retreat of critical bank near site BF3 on the Barren Fork Creek from 2008 to 2010 displayed on 2008 NAIP imagery (USDA-FSA, 2008).

A summary of the calibration data can be seen in Table 4-5. The error provides the measurement from the median value to the minimum and maximum values. Using both calibration data sets, the first CONCEPTS simulation for the reach including all six cross sections used the initial measured or calculated parameters, including the α correction factors. This simulation produced approximately 15 m of bank retreat between October 1, 2007 and October 1, 2011 (Figure 4-8), which was less than the observed retreat. For the six months of 2009 recorded by Midgley et al. (2012), the critical bank retreated at least 8 m, based on the minimum measured retreat along the 100 m measured bank. Therefore, parameter adjustments were required to match observed data.

Table 4-5. Median cumulative lateral streambank migration and error (indicating distance to minimum and maximum values) on Barren Fork Creek near the BF3 site used for CONCEPTS model calibration.

Source	*Date*	*Median Cumulative Lateral Erosion (m)*	*Error (m)*
Midgley et. al. (2012)	4/18/2009	0	0.0
	5/15/2009	5	3.1
	9/26/2009	12	4.6
	10/12/2009	15	7.3
NAIP	5/4/2008	0	0.0
	8/9/2010	20	10

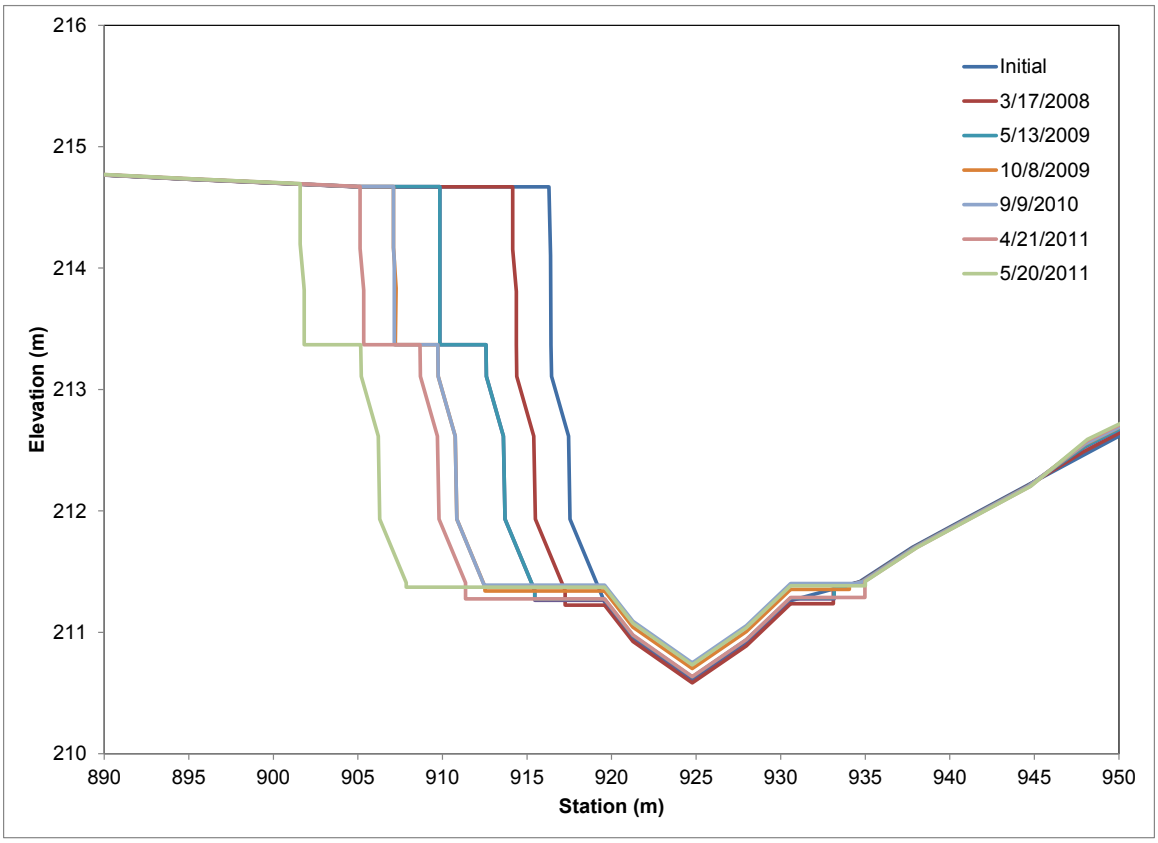

Figure 4-8. CONCEPTS predicted cross sectional changes at site BF3 with no calibration applied.

Also, based on observations, the profile of the bank was unrealistic. At the intersection of the cohesive and noncohesive layers (elevation 213.4 m) a large shelf, approximately 3 m in length, began to form where the noncohesive layer erosion did not retreat at the same rate as the cohesive layer. As illustrated in Figure 4-9, the site consistently exhibited near vertical banks, with the exception of failed material at the bank toe.

In order to simulate vertical bank profiles, τ_c of the noncohesive layer was decreased independently at each site until all six sites exhibited physically representative bank profiles. Table 4-6 shows initial and calibrated τ_c of the noncohesive layer at each site, which includes the site specific alpha correction factors. The calibrated cross sections for each site are given in Appendix D.

Figure 4-9. Example of Barren Fork Creek vertical bank face at site BF3 (Midgley et al., 2012).

Table 4-6. Initial and calibrated critical shear stress, τ_c, for noncohesive soil layers at each site in order to achieve vertical bank faces.

Site	*Initial Calculated τ_c (Pa)*	*Calibrated τ_c (Pa)*
BF1	5.5	3.0
BF2	2.2	1.0
BF3	9.7	1.5
BF4	8.4	8.0
BF5	6.0	6.0
BF6	3.5	1.0

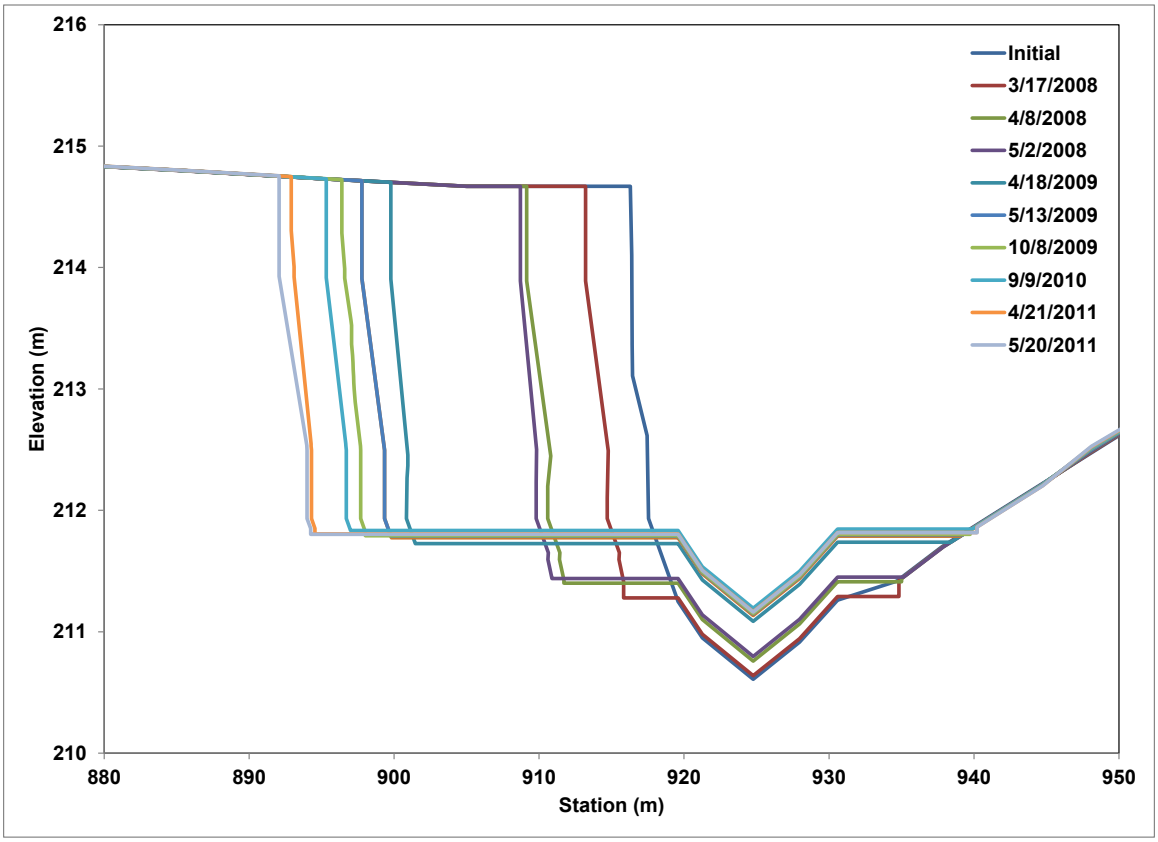

Figure 4-10. CONCEPTS output predicted cross sectional changes at site BF3 with final calibrated values.

With the calibrated site specific critical shear stresses, the simulated cross section at site BF3 was more physically accurate and matched the expected range of bank retreat (Figure 4-10). Over the four year simulation period, the critical bank at site BF3 retreated approximately 24 m. Figure 4-11 illustrates the overlap in the three sets of data.

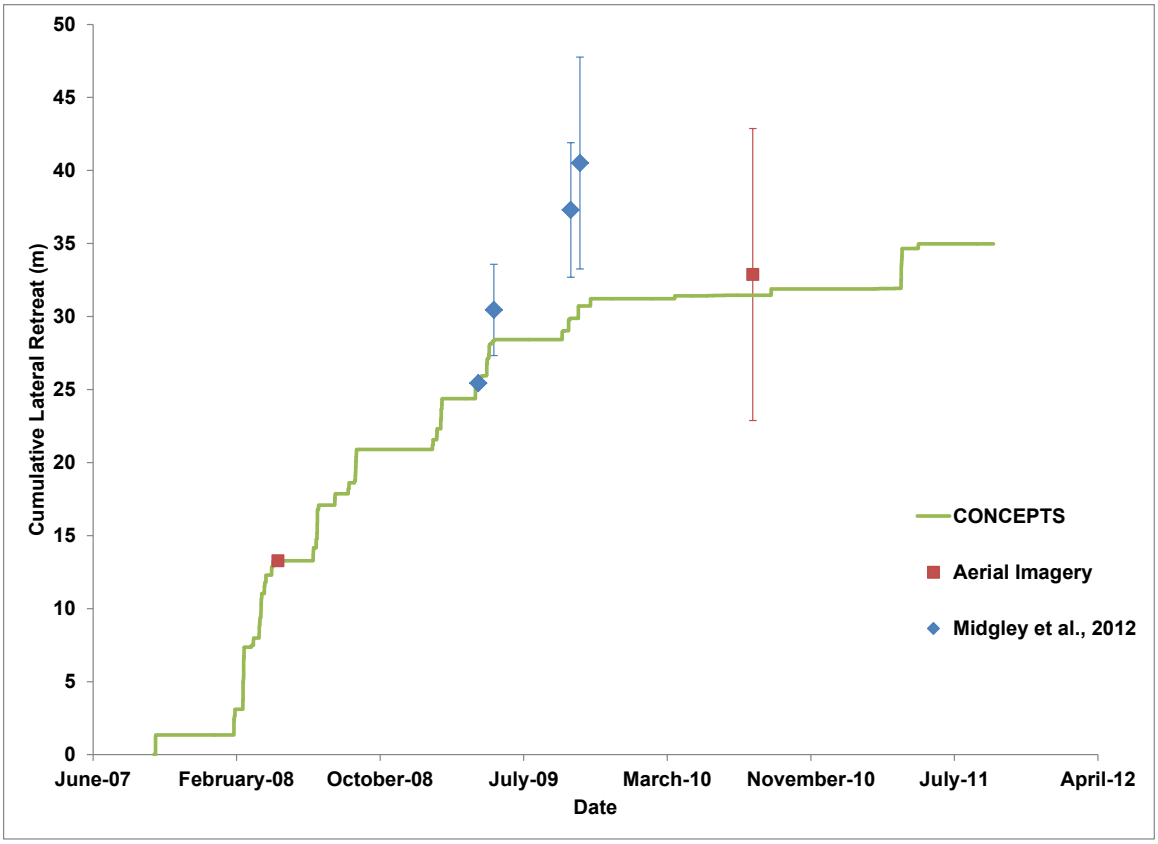

Figure 4-11. Calibrated cumulative lateral erosion as compared to aerial imagery and ground based data. Symbols represent the mean lateral retreat with error bars indicating the minimum and maximum measured retreat.

Both data sets, aerial imagery and ground based data from Midgely et al. (2012), and CONCEPTS had different starting points of 5/4/2008, 4/18/2009 and 10/1/2007, respectively. In order to compare CONCEPTS predictions with the two data sets, the initial aerial imagery and ground based data were set to the CONCEPTS simulated cumulative bank retreat at their specified start dates and then changes were recorded with respect to that measurement. It is important to note that the CONCEPTS simulated lateral bank migration and the observed data are slightly different, and thus caution should be taken when making a direct comparison. The aerial imagery and the ground based data measured cumulative lateral retreat of the critical bank, while the CONCEPTS predictions were the cumulative lateral retreat at the bank toe elevation, with respect to both the critical and noncritical banks. Since the banks are near vertical, the difference between the toe width and bank top width should be comparable; however, the CONCEPTS predictions takes into account the toe retreat of the opposite bank as well. Since the noncritical bank at this site is not degrading or aggrading at a rapid rate, the observed and predicted lateral migration rates were still relatively comparable.

The CONCEPTS predicted bank retreat compares well with the range of retreat measured with aerial imagery and reasonably well with the ground based data. In addition, the CONCEPTS predicted bank retreat follow the trend and timing of the ground-based data, but differences in measurement location and the toe and bank top elevations may account for these differences. With these limitations of calibration data, the calibration was concluded to be acceptable for the purposes of this study.

4.4 Bank Stabilization

Using CONCEPTS, a base scenario was simulated using the initial cross sections with the calibrated or measured geotechnical parameters. Two highly unstable sites from the reach were chosen to simulate stabilization practices, BF2 and BF3. Two types of stabilization practices were simulated including slope stabilization and toe protection. Slope stabilization was intended to reduce geotechnical failures while toe protection was intended to reduce fluvial erosion. Each practice was modeled by itself and in combination with the other practice.

The slope stabilization scenario consisted of reshaping the critical bank to a 2:1 slope. This was achieved in CONCEPTS by changing the cross-sectional input starting at the toe of the critical bank. The bank toe was left in its original position and the bank top was altered to create a 2:1 slope. The toe protection scenario consisted of applying a 1.5 m layer of riprap to the toe of the critical bank. This was achieved by simulating different 1.5 m soil layer on the toe of the critical bank. This layer had the same properties as the original toe layer except with alterations to the critical shear stress, particle size distribution, and friction angle in order to simulate riprap. The particle size distribution was altered to 100% finer at the small cobbles size class; the largest size class input in CONCEPTS. The critical shear stress and friction angle were estimated for 0.254 m riprap at 225 Pa and 42°, respectively (Fischenich, 2001). All scenarios were simulated using the same four-year flow record used for model calibration.

Figures 4-12 and 4-13 show the cross sectional results for the base scenario, slope stabilization scenario, toe protection scenario, and a scenario in which both toe protection and slope stabilization were simulated for sites BF2 and BF3, respectively. The sites were stabilized one at a time with one site remaining at its base calibrated scenario, while the other site was simulated with the various stabilization scenarios. Both

sites showed a decrease in lateral retreat with the slope stabilization and a halting of any toe retreat with the toe protection. For the combined toe protection and slope stabilization scenario at both sites provided minimal improvement over toe protection alone. For site BF2, there was a reduction of lateral top width retreat of 11 m using slope stabilization, 35 m using toe protection, and 33 m using both slope stabilization and toe protection. For site BF3, there was a reduction of lateral top width retreat of 5 m using slope stabilization, 8 m using toe protection, and 7 m using both slope stabilization and toe protection. Therefore, the three stabilization scenarios performed similarly at both sites but provide different results based on site specific conditions.

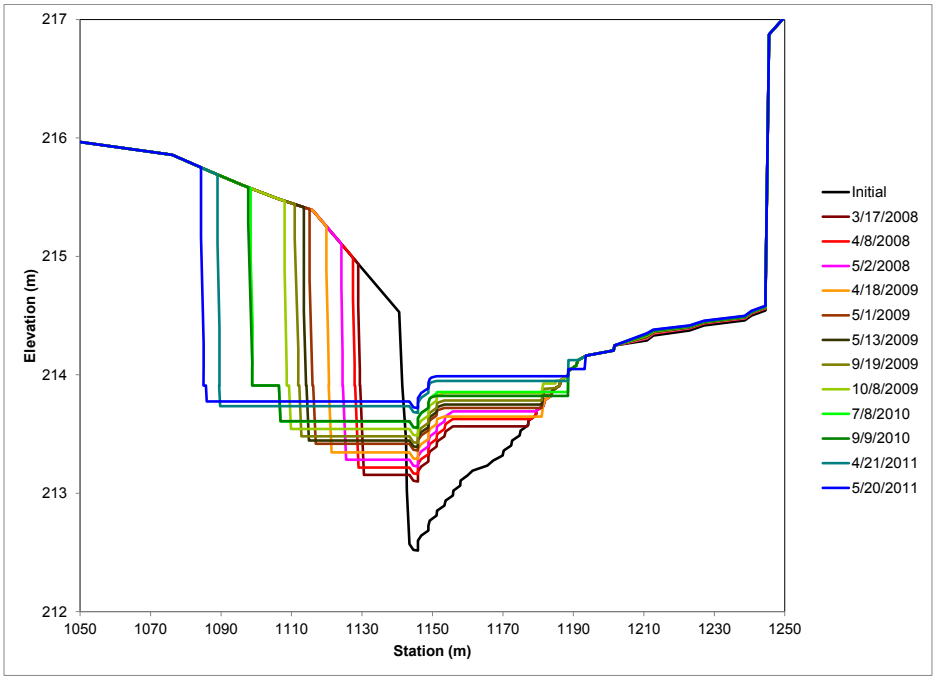

Figure 4-12a. CONCEPTS predicted cross sectional changes at site BF2 for the base scenario.

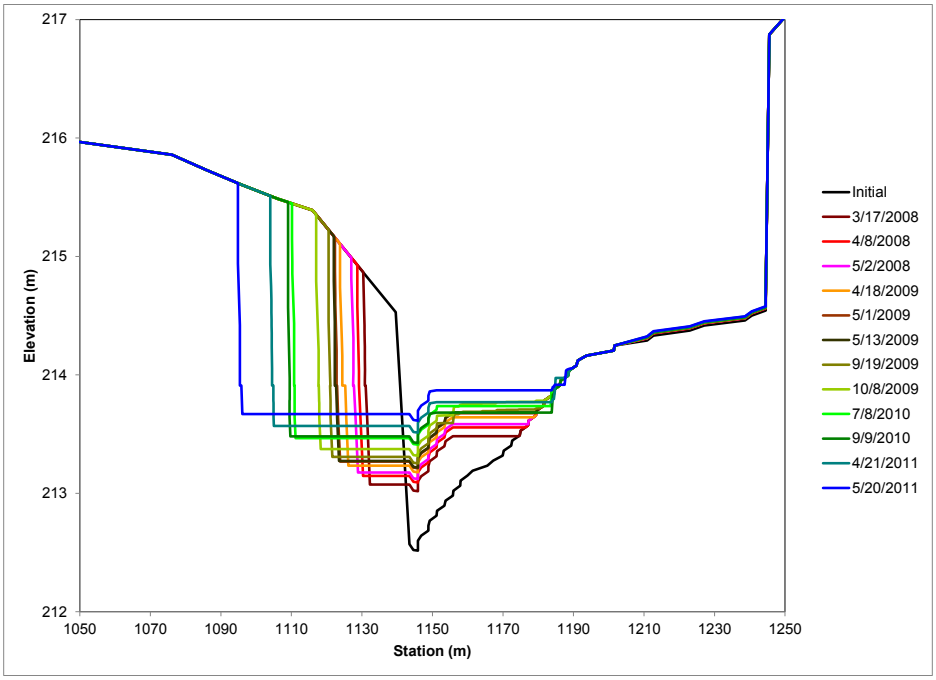

Figure 4-12b. CONCEPTS predicted cross sectional changes at site BF2 for the slope stabilization scenario.

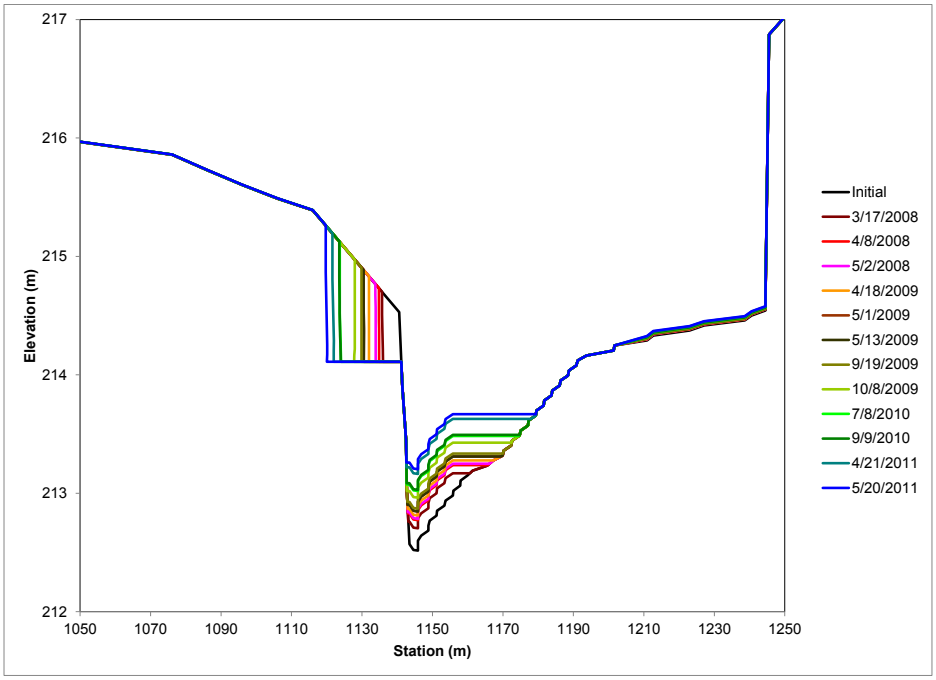

Figure 4-12c. CONCEPTS predicted cross sectional changes at site BF2 for the toe protection scenario.

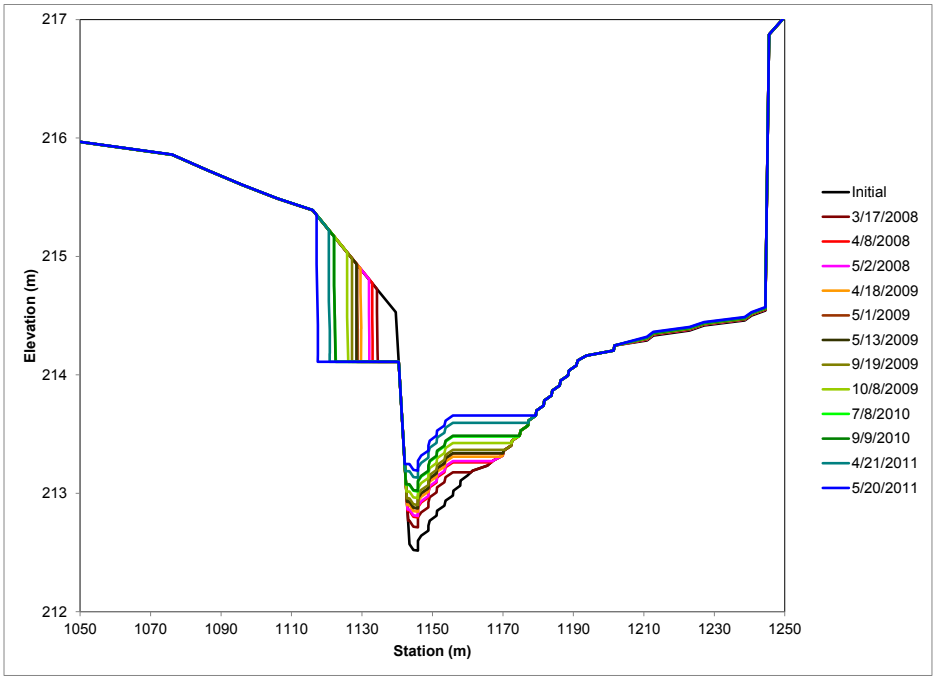

Figure 4-12d. CONCEPTS predicted cross sectional changes at site BF2 for the combination slope stabilization and toe protection scenario.

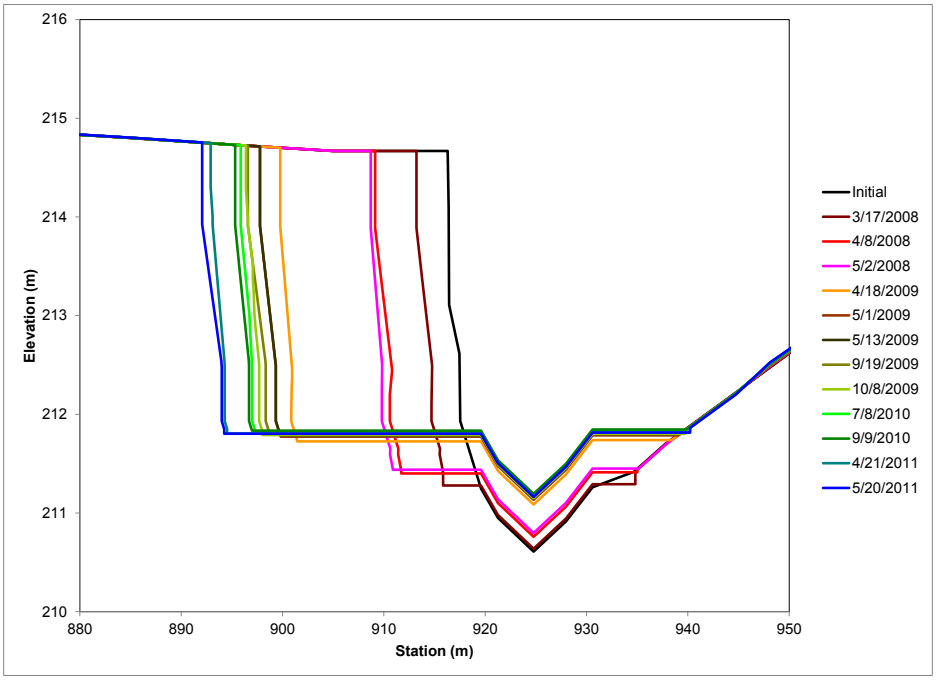

Figure 4-13a. CONCEPTS predicted cross sectional changes at site BF3 for the base scenario.

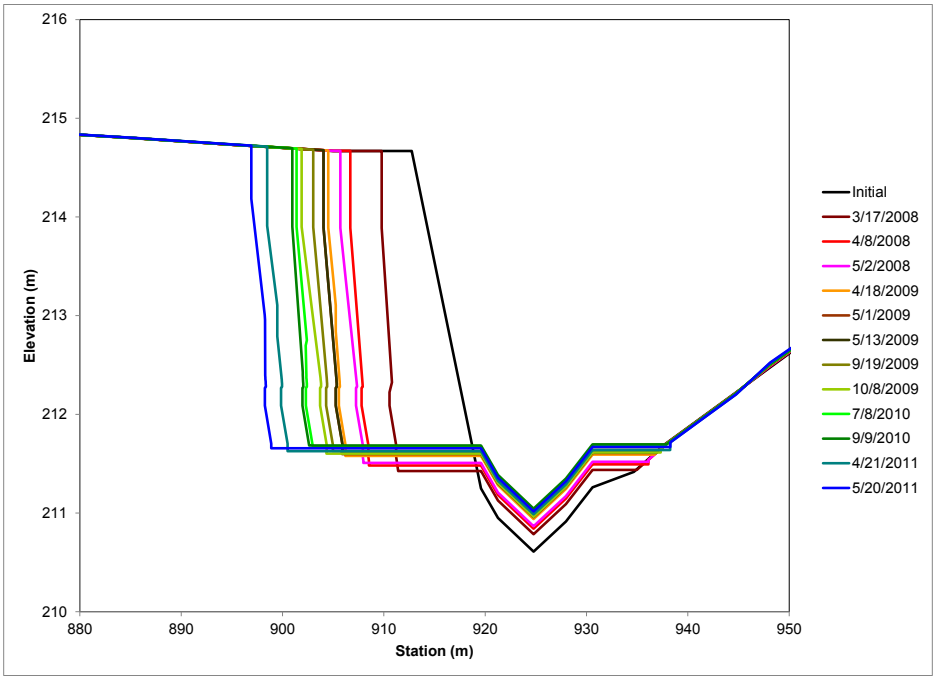

Figure 4-13b. CONCEPTS predicted cross sectional changes at site BF3 for the slope stabilization scenario.

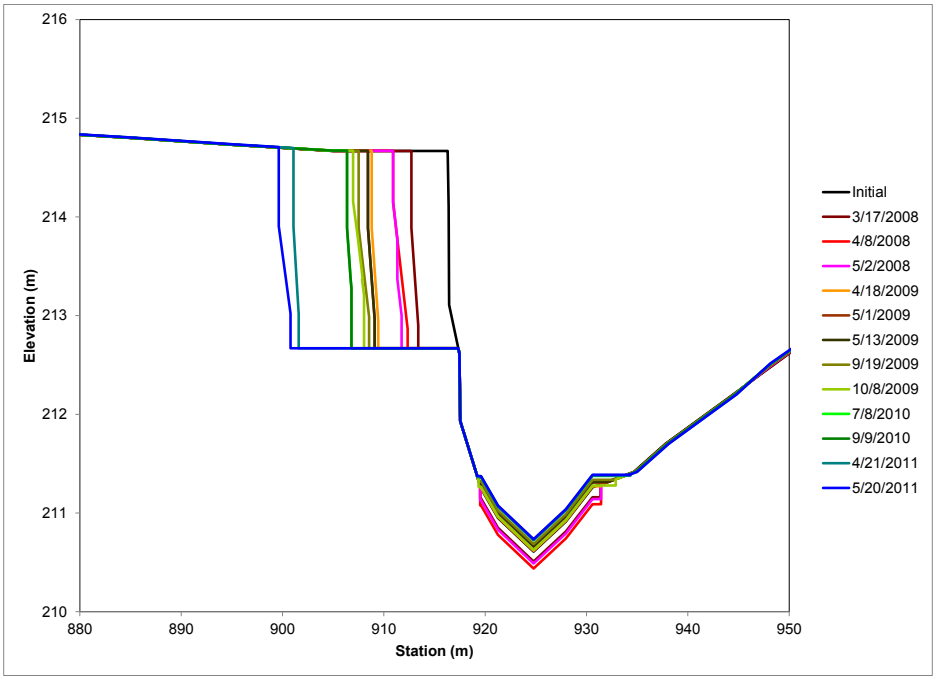

Figure 4-13c. CONCEPTS predicted cross sectional changes at site BF3 for the toe protection scenario.

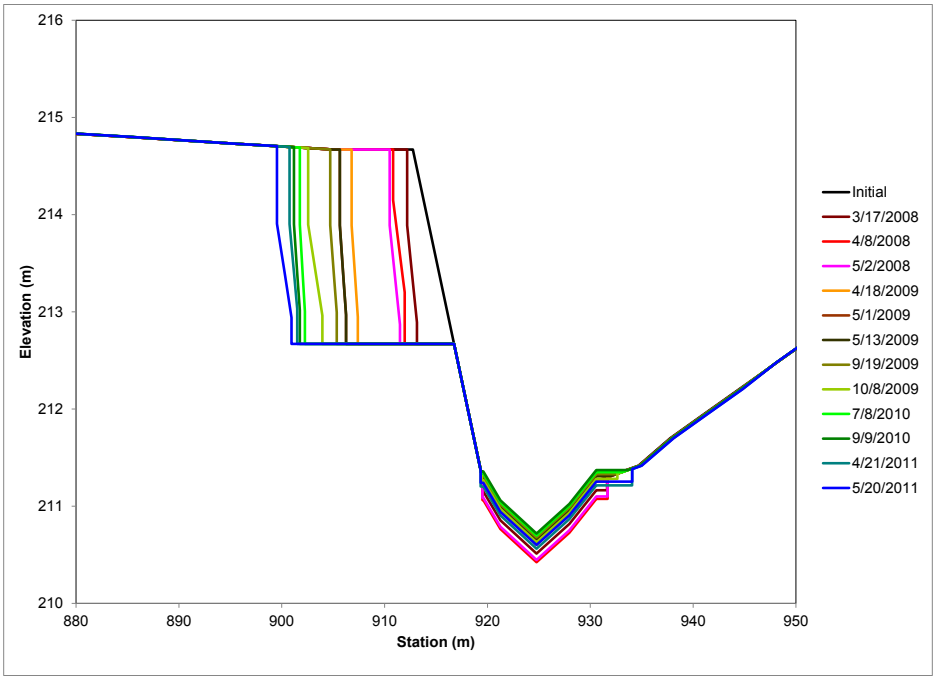

Figure 4-13d. CONCEPTS predicted cross sectional changes at site BF3 for the combination slope stabilization and toe protection scenario.

Cross sectional changes illustrated the ability of stabilization procedures to reduce bank retreat; an alternative assessment was evaluating sediment load reductions. Figure 4-14 shows the percent reduction in cumulative fines, cumulative lateral erosion at the bank toe and top, and the cumulative change in bed elevation over the four year simulation for sites BF2 and BF3. These results vary for each site. Site BF2 showed an overall percent reduction in fines while site BF3 showed an increase in yield for fines when toe protection was used. This implies that utilizing toe protection at site BF3 actually caused an increase in sediment yield compared to an unstabilized site. This may be a result of the riprap layer thickness at this site. Both sites received a layer of riprap on the bottom 1.5 m of their banks. At site BF2, this was a large enough layer to cover the entirety of the noncohesive layer and a small portion of the cohesive layer, but at site BF3 this covered less than three quarters of the noncohesive layer and none of

the cohesive layer. This may have caused additional undercutting, and therefore mass failures due to the exposed gravel and cohesive layers (Figure 4-15).

Based on these percent fines reductions, both slope stabilization and toe protection in combination provide the best measure of stabilization for site BF3 and toe protection alone or coupled with slope stabilization provide the best measure of stabilization for site BF2. In addition, it was more beneficial to stabilize site BF2 over site BF3 if only one site can be chosen. This is because of the overall decrease in sediment yield and lateral erosion seen at site BF2.

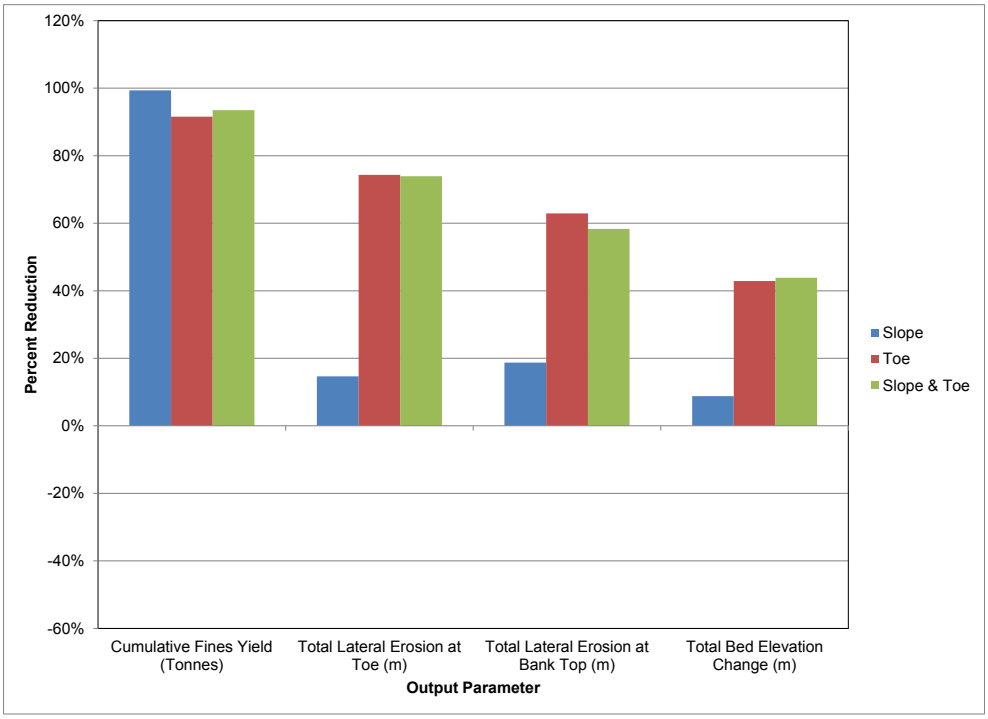

Figure 4-14a. CONCEPTS predicted percent sediment reductions for site BF2 for the slope stabilization, toe protection, and combination slope stabilization and toe protection stabilization scenarios.

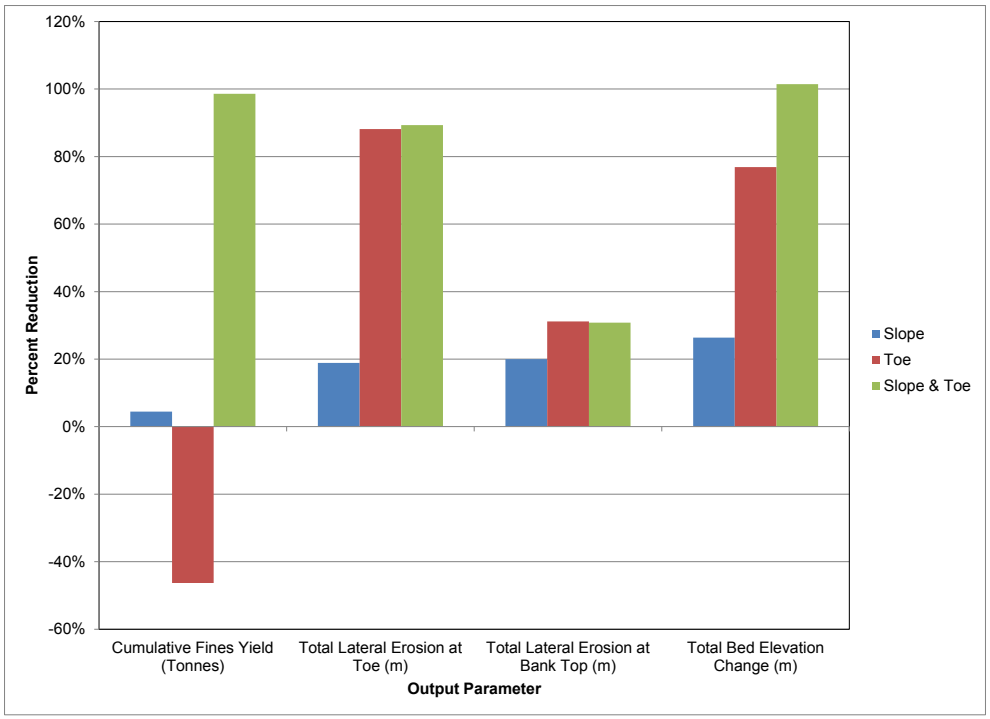

Figure 4-14b. CONCEPTS predicted percent sediment reductions for site BF3 for the slope stabilization, toe protection, and combination slope stabilization and toe protection stabilization scenarios.

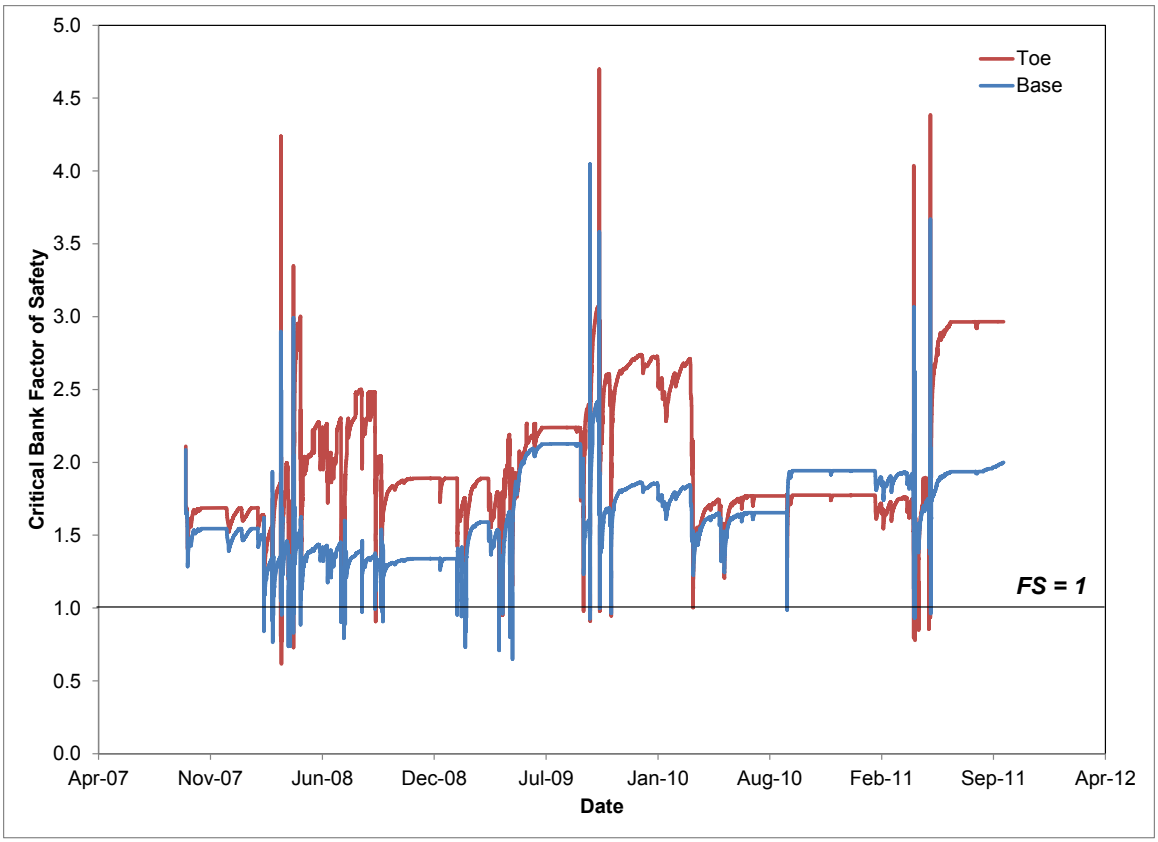

Figure 4-15. CONCEPTS predicted factor of safety (FS) of the critical bank at BF3 for the base scenario and toe protection stabilization scenario.

Stabilization projects have the potential to affect the entire reach and not just the site where the project was implemented. By reducing sediment loads entering the stream and any channel widening and deposition that may occur at the stabilization site, effects can spread both upstream and downstream. It is important to consider these repercussions when choosing a site to stabilize. Although there may be localized benefits at the stabilization site, the upstream and downstream effects may outweigh the benefits in the long term by causing additional erosion or scouring at other sites. Figure 4-16 illustrate this point by presenting the changes in cumulative fines yield at each site with respect to the site stabilized and the type of stabilization implemented.

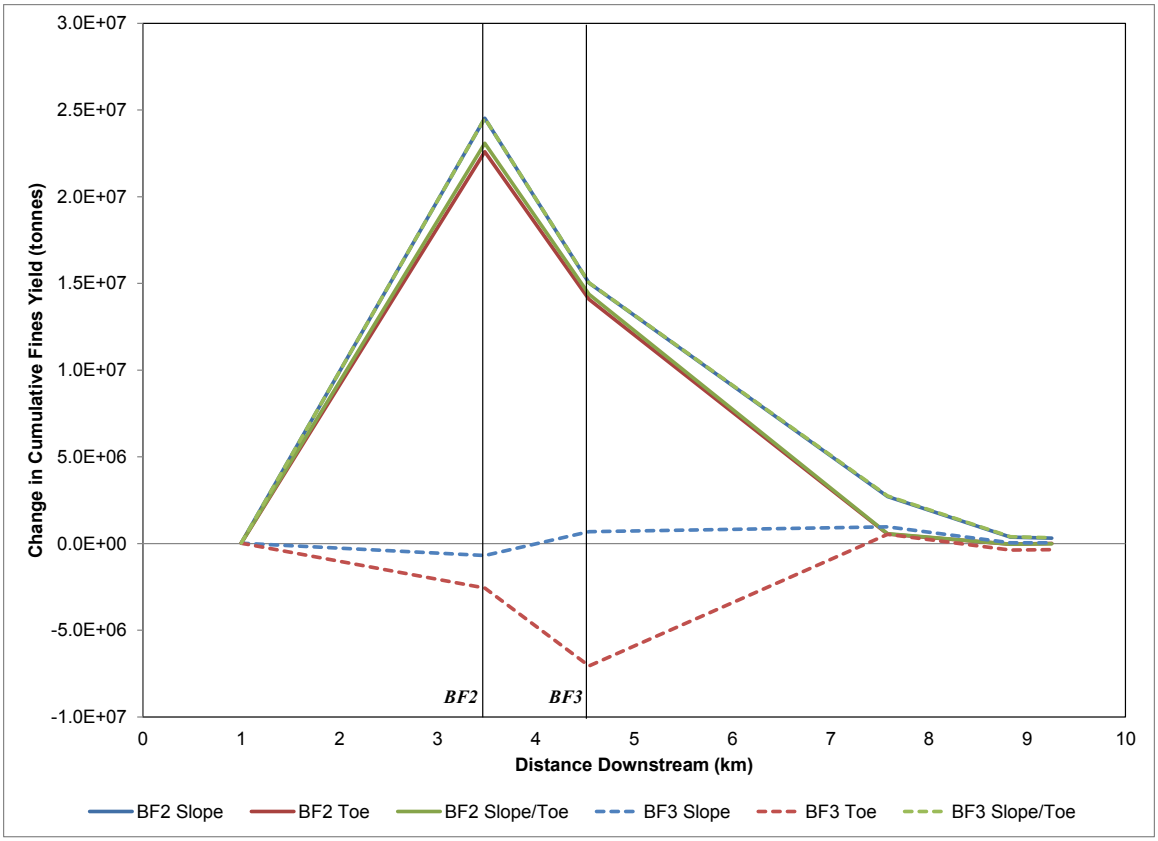

Figure 4-16. CONCEPTS predicted change in cumulative yield for fines for the slope stabilization, toe protection, and combination slope stabilization and toe protection stabilization scenarios.

From Figure 4-16 it is evident that alterations at BF2 caused significantly less fines movement directly downstream. Alterations at site BF3 caused a decrease in fines movement downstream and an increase in fines movement upstream due toe protection. As shown in Figure 4-17, based on the cumulative change in the thalweg elevation, the alterations at BF2 and BF3 both caused less deposition on the bed, scouring in some places, and increased deposition in others. Although no headcut is evident yet, these scoured areas may lead to headcuts in the future which may cause increased incision and decreased bank stability.

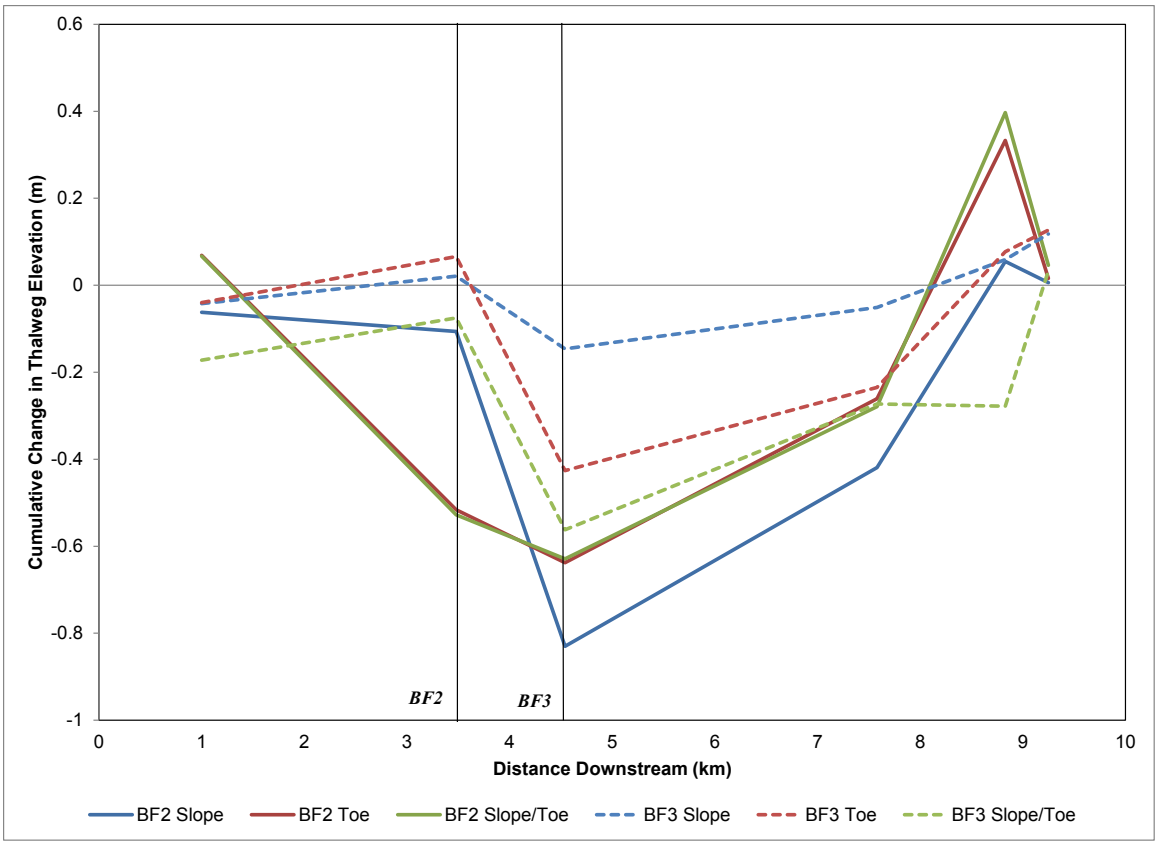

Figure 4-17. CONCEPTS predicted change in cumulative thalweg elevation along the simulated reach for the slope stabilization, toe protection, and combination slope stabilization and toe protection stabilization scenarios.

CHAPTER V

SUMMARY AND CONCLUSIONS

The objective of this study was to perform an evaluation of CONCEPTS as applied to composite streambanks along Barren Fork Creek in the Ozark Highlands ecoregion and to demonstrate CONCEPTS's ability to model long-term streambank stabilization procedures on these composite banks for use as a management tool for future stabilization projects. In order to meet this objective, three sub-objectives were outlined and included performing a sensitivity analysis, performing a model calibration, and applying bank stabilization procedures to predict the long term success of stabilization projects. Each step in this three step process produced a wealth of information about CONCEPTS as a stabilization model and management tool, important issues in streambank modeling, and gaps that exist in streambank research.

The sensitivity analysis identified the CONCEPTS parameters that were the most sensitive to streambank erosion. The two most sensitive parameters were the friction angle and the alpha value. The alpha value was estimated using the RVR Meander model and the CONCEPTS relative sensitivity coefficient may be a function of the limitations of RVR Meander. The alpha values were based on bankfull flow and a constant channel width and depth. In reality, all three of these parameters change with

flow and would ideally be incorporated into CONCEPTS and updated based on flow and channel geometry. With the current limitation of alpha, CONCEPTS may over predict fluvial erosion during low flow events and under predict fluvial erosion during high flow events. In addition, the alpha value was only applied to the critical bank in this study. In principle, an alpha value should be calculated separately for the critical and non-critical banks, which would more precisely model the effects of aggradation on the inside of a meander bend and degradation on the outside of the meander bend. The alpha value of the non-critical bank, or inside of a meander bend, would be calculated as less than one with the applied shear stress at the bank being less than the centerline applied shear stress. Conversely, and as seen in this study, the alpha value of the critical bank, or the outside of a meander bend, would be calculated as greater than one with the applied shear stress at the bank being greater than that at the centerline. Because bank erosion was shown to be quite sensitive to the assigned alpha values, a more comprehensive approach to assigning them at each site should be considered. This also calls attention to the need of two-dimensional or three-dimensional models in this field of study.

The sensitivity analysis also identified the internal angle of friction as a highly sensitive parameter for bank erosion. The internal angle of friction had a different impact based on whether the soil was cohesive or noncohesive. The cohesive soils had an internal angle of friction that was measured *in situ*, and the angle of repose based on mean particle diameter was used for the noncohesive soils. This was suitable for noncohesive soils that were loose and had negligible interstitial cohesion; however the gravels in this system were packed gravels that may have some cohesion that was not being accounted for using this method. Millar (2005) also suggested that the internal angle of friction for these soils may act as a lumped calibration parameter that accounts for several physical processes. At the moment, these processes are not being simulated

but have been shown to be extremely important through the high relative sensitivity of the internal angle of friction. More research is needed on the internal angle of friction and its role in packed gravel systems.

These issues and others were also evident through the CONCEPTS model calibration process. The initial predicted eroded profiles using measured data and the correction for channel sinuosity, produced unrealistic profile shapes forming a horizontal shelf at the intersection of the cohesive and noncohesive layers. This issue was fixed by altering, drastically in some cases, the critical shear stresses of the noncohesive layers in order to achieve the observed near vertical bank profiles. While this approach created realistic profiles, it focused on modifying parameters for the fluvial erosion component and may have overestimated fluvial erosion when the actual issue may have been with the bank stability component. CONCEPTS assumed a hydrostatic groundwater pressure in the streambank that changed linearly with depth from the top of the bank. This assumption may have created additional apparent cohesion on the noncohesive layer that was not present in reality, but helped to simulate near vertical banks. The bottom layer and toe of the bank were expected to drain quickly during drawdown conditions leaving a saturated, heavy cohesive layer at the top of the bank susceptible to failure. This may not have been captured accurately within the CONCEPTS simulations, and thus may have largely underestimated mass failures within the cohesive layers and overestimated fluvial erosion within the noncohesive layers.

These limitations may, in turn, have effected predictions when simulating different stabilization methods. If fluvial erosion or mass failures were underestimated or overestimated, stabilization procedures targeting one or both of these erosion mechanisms may not be simulated properly. For example, stabilization projects may be targeted for decreasing fluvial erosion if mass failures were underestimated, when in

reality the dominant erosional process may, in fact, have been mass failure. Predictions from the different stabilization techniques simulated in this study identify this issue as a possible reason for discrepancies between similar sites and the predicted eroded profiles after stabilization techniques were simulated.

Based on the above observations, it was concluded that, with proper estimates and measurements of physical data and proper calibration, CONCEPTS could be a valuable tool for watershed managers to prioritize and select suitable streambank stabilization sites. However, significant gaps exist in estimating physical parameters for noncohesive soils and the effects that certain parameters have on streambank stability predictions. Although additional research is needed to address parameter estimation and calibration issues, CONCEPTS is a viable tool to consider when investigating the long-term effects of a stabilization project on a reach scale.

REFERENCES

Abad, J.D., and M.H. Garcia. 2006. RVR Meander: A toolbox for re-meandering of channelized streams. Computers & Geosciences 32 (1): 92-101. doi:10.1016/j.cageo.2005.05.006.

Al-madhhachi, A.T., G.J. Hanson, G.A. Fox, A.K. Tyagi, and R. Bulut. Measuring erodibility of cohesive soils using laboratory jet erosion tests. Proceedings from the World Environmental and Water Resources Congress 2011: Bearing Knowledge for Sustainability. Palm Springs, CA.

Camporeale, C., P. Perona, A. Porporato, and L. Ridolfi. 2007. Hierarchy of models for meandering rivers and related morphodynamic processes. Reviews of Geophysics 45 (1). doi: 10.1029/2005rg000185.

Cancienne R.M., G.A. Fox, and A. Simon. 2008. Influence of seepage undercutting on the stability of root-reinforced streambanks. Earth Surface Processes and Landforms 33 (1): 1769-1786. doi: 10.1002/esp.1657.

Crosato, A. 2009. Physical explanations of variations in river meander migration rates from model comparison. Earth Surface Processes and Landforms 34: 2078-2086. doi: 10.1002/esp.1898

Fox, G.A. and G.V. Wilson. 2010. The role of subsurface flow in hillslope and stream bank erosion: a review. Soil Science Society of America Journal 74 (1): 717-733. doi: 10.2135/sssaj2009.0319.

Fischenich, C. 2001. Stability thresholds for stream restoration materials. EMRRP Technical Notes Collection (ERDC TN-EMRRP-SR-29), U.S. Army Engineer Research Development Center, Vicksburg, MS.

FISRWG. 1998. Stream Corridor Restoration: Principles, Processes, and Practices. By the Federal Interagency Stream Restoration Working Group (FISRWG) (15 Federal agencies of the US gov't). GPO Item No. 0120-A; SuDocs No. A 57.6/2:EN 3/PT.653. ISBN-0-934213-59-3.

Fuchs, J.W., G.A. Fox, D.E. Storm, C.J. Penn, and G.O. Brown. 2009. Subsurface transport of phosphorus in riparian floodplains: Influence of preferential flow paths. Journal of Environmental Quality 38 (2): 473-484. doi:10.2134/Jeq2008.0201.

Haan, C.T., B. Allred, D.E. Storm, G.J. Sabbagh, and S. Prabhu. 1995. Statistical procedure for evaluating hydrologic / water quality models. Transactions of the ASAE 38 (3): 725-733.

Hanson, G.J., K.M. Robinson, D.M. 1990. Pressure and stress distributions due to a submerged impinging jet. ASCE National Conference on Hydraulic Engineering, New York: 252−530.

Hanson, G.J., and A. Simon. 2001. Erodibility of cohesive streambeds in the loess area of the Midwestern USA. Hydrological Processes 15 (1):23-38.

Hanson, G.J., and K.R. Cook. 2004. Apparatus, test procedures, and analytical methods to measure soil erodibility in situ. Applied Engineering in Agriculture 20 (4):455-462.

Hanson, G.J., and S.L. Hunt. 2009. Mini-JET test predicts erodibility " Agricultural Research no. 57 (9):23.

Heeren, D.M., G.A. Fox, D.E. Storm, P.Q. Storm, B.E. Haggard, T. Halihan, and R.B. Miller. 2012. Quantification and heterogeneity of infiltration and transport in alluvial floodplains. ASABE Annual International Meeting. Dallas, TX: ASABE.

Lane, E.W. 1955. Design of stable channels. Transactions of the American Society of Civil Engineers (ASCE) 120:1234 - 1260.

Langendoen, E.J. 2000. CONCEPTS - Conservational Channel Evolution and Pollutant Transport System, Stream Corridor Version 1.0. edited by U.S. Department of Agriculture Agricultural Research Service. Oxford, MS: National Sedimentation Laboratory.

Langendoen, E.J. and A. Simon. 2008. Modeling the evolution of incised streams. II: Streambank erosion. Journal of Hydraulic Engineering 134 (7): 905 – 915. doi: 10.1061/(ASCE)0733-9429(2008)134:7(905).

Langendoen, E.J. and A. Simon. 2009. Closure to “modeling the evolution of incised streams. II: streambank erosion”. Journal of Hydraulic Engineering 135: 1107 – 1108.

Midgley, T.L., G.A. Fox, and D.M. Heeren. 2012. Evaluation of the bank stability and toe erosion model (BSTEM) for predicting lateral retreat on composite streambanks. Geomorphology 145-146:107-114.

Millar, R.G. 2000. Influence of bank vegetation on alluvial channel patterns. Water Resources Research 36(4):1109-1118. Paper number 1999WR900346.

Millar, R.G. 2005. Theoretical regime equations for mobile gravel-bed rivers with stable banks. Geomorphology 64 (3-4):207-220. doi:10.1016/j.geomorph.2004.07.001.

Motta, D., J.D. Abad, E.J. Langendoen, and M.H. Garcia. 2012. A simplified 2D model for meander migration with physically-based bank evolution. Geomorphology 163:10-25. doi: 10.1016/j.geomorph.2011.06.036.

Oklahoma Conservation Commission (OCC). 2010. Watershed Based Plan for the Illinois River Watershed. OCC Water Quality Division. Oklahoma City, OK.

Rinaldi, M., B. Mengoni, L. Luppi, S.E. Darby, and E. Mosselman. 2008. Numerical simulation of hydrodynamics and bank erosion in a river bend. Water Resources Research 44 (9). doi: 10.1029/2008wr007008.

Rousselot, P. 2009. Discussion of “modeling the evolution of incised streams. II: streambank erosion”. Journal of Hydraulic Engineering 135: 1107 – 1108.

Shields, F.D., R.R. Copeland, P.C. Klingeman, M.W. Doyle, and A. Simon. 2003. Design for stream restoration. Journal of Hydraulic Engineering 129 (8): 575-584. doi: 10.1061/(ASCE)0733-9429(2003)129:8(575).

Simon, A. 1989. A model of channel response in disturbed alluvial channels. Earth Surface Processes and Landforms 14: 11-26.

Simon, A., and P.W. Downs. 1995. An interdisciplinary approach to evaluation of potential instability in alluvial channels. Geomorphology 12 (3):215-232.

Simon, A., A. Curini, S.E. Darby, and E.J. Langendoen. 2000. Bank and near-bank processes in an incised channel. Geomorphology 35 (3-4):193-217.

Simon, A., Thomas, R., Curini, A., and N. Bankhead. 2001. Bank Stability and Toe Erosion Model. Static Version 5.2.

Simon, A., and M. Rinaldi. 2006. Disturbance, stream incision, and channel evolution: The roles of excess transport capacity and boundary materials in controlling channel response. Geomorphology 79 (3-4):361-383. doi:10.1016/j.geomorph.2006.06.037.

USDA-FSA Aerial Photography Field Office. 2008. National Agriculture Imagery Program (NAIP). Vector digital data. Salt Lake City, Utah.

USDA-FSA Aerial Photography Field Office. 2010. National Agriculture Imagery Program (NAIP). Vector digital data. Salt Lake City, Utah.

White, K.L. and I. Chaubey. 1995. Sensitivity analysis, calibration, and validations for a multisite and multivariable SWAT model. Journal of the American Water Resources Association (JAWRA) 41(5): 1077-1089.

Wolman, M.G. 1954. A method of sampling coarse river-bed material." Transactions of the American Geophysical Union 35 (6):951-956.

APPENDICES

Appendix A: Data Collection Packet

Appendix B: CONCEPTS Input Data

Appendix C: RVR Meander Output

Appendix D: Output Calibrated Cross Sections

APPENDIX A

PEBBLE COUNT (PC)
Field Data Sheet

SITE:	
DATE:	**PERSONNEL:**
PC Location: Bed Bank	**Comments:**

1 _____	21 _____	41 _____	61 _____	81 _____
2 _____	22 _____	42 _____	62 _____	82 _____
3 _____	23 _____	43 _____	63 _____	83 _____
4 _____	24 _____	44 _____	64 _____	84 _____
5 _____	25 _____	45 _____	65 _____	85 _____
6 _____	26 _____	46 _____	66 _____	86 _____
7 _____	27 _____	47 _____	67 _____	87 _____
8 _____	28 _____	48 _____	68 _____	88 _____
9 _____	29 _____	49 _____	69 _____	89 _____
10 _____	30 _____	50 _____	70 _____	90 _____
11 _____	31 _____	51 _____	71 _____	91 _____
12 _____	32 _____	52 _____	72 _____	92 _____
13 _____	33 _____	53 _____	73 _____	93 _____
14 _____	34 _____	54 _____	74 _____	94 _____
15 _____	35 _____	55 _____	75 _____	95 _____
16 _____	36 _____	56 _____	76 _____	96 _____
17 _____	37 _____	57 _____	77 _____	97 _____
18 _____	38 _____	58 _____	78 _____	98 _____
19 _____	39 _____	59 _____	79 _____	99 _____
20 _____	40 _____	60 _____	80 _____	100 _____

PC: _____% **PS:**_____%

SITE SKETCH

Nov. 4 2011

JET EROSION TEST (JET)
Field Data Sheet

SITE:						
DATE:			PERSONNEL:			
Test #:	Weather:		Bank Material:			
Test Type:	JET	Mini-JET	Test Location:	Bed	Bank Toe	Bank Face

	PT GAUGE READING PRIOR TO WETTING (MM)	PRELIMINARY HEAD SETTING (PSI)	

SCOUR DEPTH READINGS		
TIME (MIN)	DIFF TIME (MIN)	PT GAUGE READING (MM)

HEAD SETTING	
TIME (MIN)	NET HEAD (PSI)

COMMENTS:

SUMMARY:

GRAPH RESULTS ON BACK

Nov. 4 2011

JET DATA GRAPH

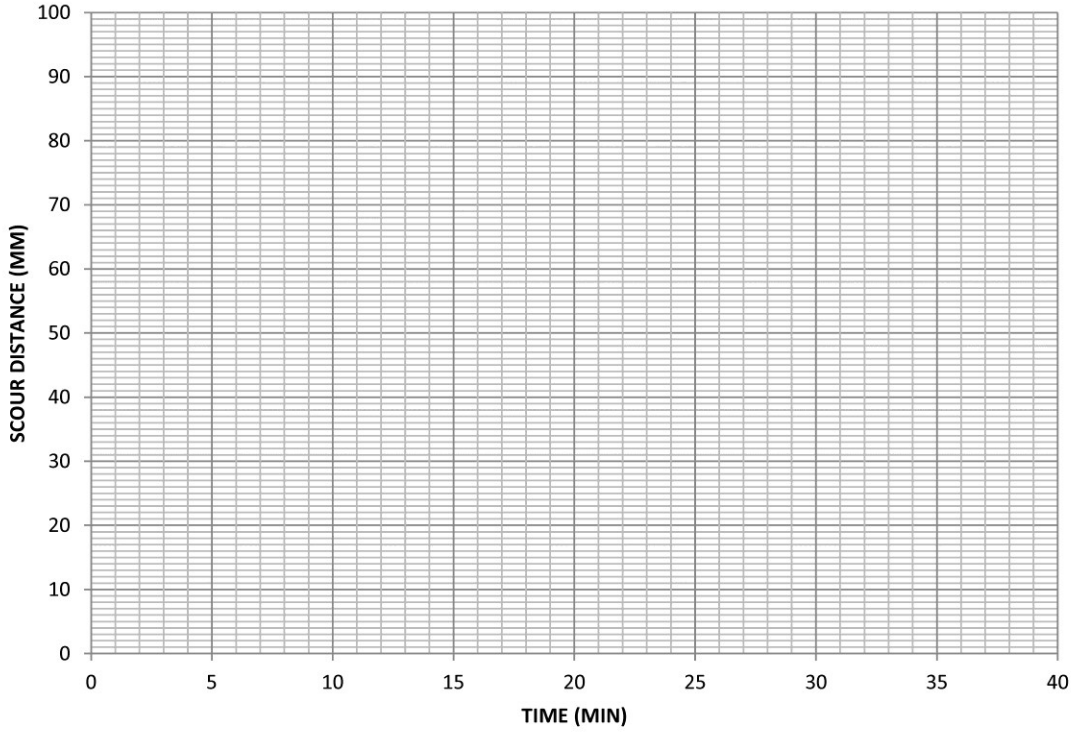

TEST SKETCH	*BANK STRATIGRAPHY*

Nov. 4 2011

BOREHOLE SHEAR TEST (BST)

Field Data Sheet

SITE:	
DATE:	**PERSONNEL:**
BST Serial #:	**Boring ID #:**
Units: kPa psf ksf psi	**Shear Head Depth:**
Shear Head Orientation: Parallel Perpendicular	**Bank Material:** Clay Silt Sand
Layer #/#:	**Weather:**
***Comments*:**	

Start Time:	**Pulls**									
	1	2	3	4	5	6	7	8	9	10
Time										
Consolidation (min)										
Normal Stress										
Shear Stress (gauge)										
Tare (pull rods)										
Soil Shear Stress										
Condition of Boring										

***SUMMARY*:**

Condition of Boring: 1 – dry, 2 – moist, 3 – submerged

GRAPH RESULTS ON BACK

Nov. 4 2011

BST DATA GRAPH

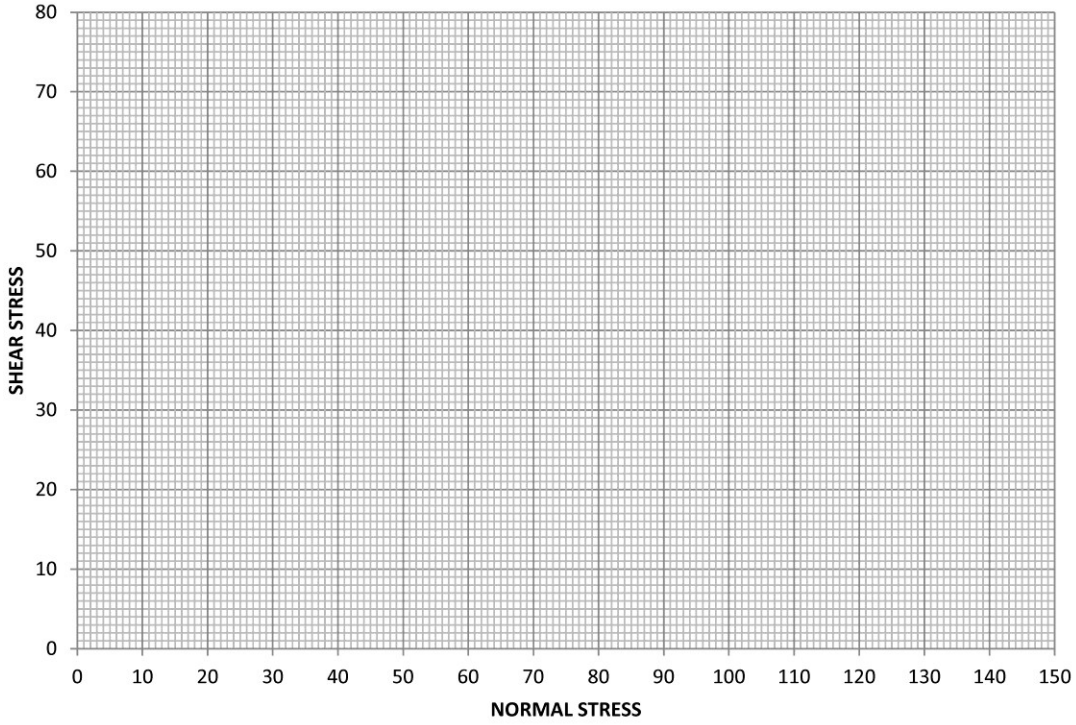

TEST SKETCH	*BANK STRATIGRAPHY*

Nov. 4 2011

CHANNEL STABILITY INDEX (CSI)
Field Data Sheet

SITE:	
DATE:	PERSONNEL:

1. Primary bed material

Bedrock	Boulder/Cobble	Gravel	Sand	Silt Clay	
0	1	2	3	4	

2. Bed/bank protection

Yes	No	(with)	1 bank	2 banks	
0	1		2	3	

3. Degree of incision (relative elevation of "normal" low water; floodplain/terrace @ 100%)

0-10%	11-25%	26-50%	51-75%	76-100%	
4	3	2	1	0	

4. Degree of constriction (relative decrease in top-bank width from up to downstream)

0-10%	11-25%	26-50%	51-75%	76-100%	
0	1	2	3	4	

5. Stream bank erosion (each bank)

	None	Fluvial	Mass Wasting (failures)	
Left	0	1	2	
Right	0	1	2	

6. Stream bank instability (percent of each bank failing)

	0-10%	11-25%	26-50%	51-75%	76-100%	
Left	0	0.5	1	1.5	2	
Right	0	0.5	1	1.5	2	

7. Established riparian woody-vegetative cover (each bank)

	0-10%	11-25%	26-50%	51-75%	76-100%	
Left	2	1.5	1	0.5	0	
Right	2	1.5	1	0.5	0	

8. Occurrence of bank accretion (percent of each bank with fluvial deposition)

	0-10%	11-25%	26-50%	51-75%	76-100%	
Left	2	1.5	1	0.5	0	
Right	2	1.5	1	0.5	0	

9. Stage of channel evolution

I	II	III	IV	V	VI	
0	1	2	4	3	1.5	

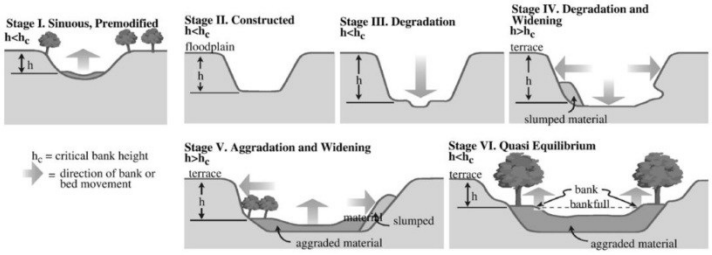

TOTAL RANK	

Nov. 4 2011

CHANNEL CROSS SECTION
Field Data Sheet

SITE:	
DATE:	**PERSONNEL:**

DISTANCE	HEIGHT
Circle one (m) (ft)	Circle one (m) (ft)

Height of Instrument:	**Photo #s:**

Survey Sketch:

Comments:

Nov. 4 2011

APPENDIX B

Site	Critical Bank	Layer Depth (m)	Layer Type	Bulk Density (kg/m^3)	Particle Density (kg/m^3)	Porosity	Permeability	Alpha	Critical Shear Stress (Pa)	Erodibility (m/s-Pa)	Cohesion (Pa)	Friction Angle (degree)	Suction Angle (degree)
BF1	L	0 - 0.2	Cohesive	1712.5	2650	0.35	4.00E-05	1.00	0.08	5.87E-06	0	28.7	15
BF1	L	0.2 - 0.4	Noncohesive	2038.7	2650	0.23	2.00E-03	1.00	3.00	1.00E-01	0	32.8	15
BF1	L	0.4 - 1.4	Cohesive	1712.5	2650	0.35	4.00E-05	1.00	0.08	5.87E-06	0	28.7	15
BF1	L	1.4 - ??	Noncohesive	2038.7	2650	0.23	2.00E-03	1.00	3.00	1.00E-01	0	32.8	15
BF1	L	-	Bed	2038.7	2650	0.23	2.00E-03	1.00	15.41	1.00E-01	0	36.3	15
BF2	L	0.0 - 0.62	Cohesive	1841.5	2650	0.31	4.00E-05	1.89	0.09	3.17E-06	1300	28.5	15
BF2	L	0.62 -	Noncohesive	2038.7	2650	0.23	2.00E-03	1.89	1.00	1.00E-01	0	31.6	15
BF2	L	-	Bed	2038.7	2650	0.23	2.00E-03	1.89	20.56	5.29E-02	0	37.9	15
BF3	L	0 - 1.3	Cohesive	1812.4	2650	0.32	4.00E-05	1.26	0.11	6.30E-06	4830	22.5	15
BF3	L	1.3 -	Noncohesive	2038.7	2650	0.23	2.00E-03	1.26	1.50	1.00E-01	0	36.9	15
BF3	L	-	Bed	2038.7	2650	0.23	2.00E-03	1.26	16.86	7.94E-02	0	36.8	15
BF4	R	0.0 - 0.97	Cohesive	1801.2	2650	0.32	4.00E-05	1.07	0.32	1.86E-06	0	36.0	15
BF4	R	0.97 -	Noncohesive	2038.7	2650	0.23	2.00E-03	1.07	8.00	1.00E-01	0	35.3	15
BF4	R	-	Bed	2038.7	2650	0.23	2.00E-03	1.07	9.08	9.31E-02	0	33.0	15
BF5	L	0.0 -	Noncohesive	2038.7	2650	0.23	2.00E-03	1.56	6.00	1.00E-01	0	35.5	15
BF5	L	-	Bed	2038.7	2650	0.23	2.00E-03	1.56	19.08	6.43E-02	0	37.5	15
BF6	L	0.0 - 0.5	Cohesive	1834.9	2650	0.31	4.00E-05	1.89	0.07	5.23E-06	0	27.0	15
BF6	L	0.5 - 1.63	Noncohesive	2038.7	2650	0.23	2.00E-03	1.89	1.00	1.00E-01	0	33.9	15
BF6	L	1.63 - 1.95	Cohesive	1834.9	2650	0.31	4.00E-05	1.89	0.07	5.23E-06	0	27.0	15
BF6	L	1.95 -	Noncohesive	2038.7	2650	0.23	2.00E-03	1.89	1.00	1.00E-01	0	33.7	15
BF6	L	-	Bed	2038.7	2650	0.23	2.00E-03	1.89	27.08	5.29E-02	0	38.7	15

Site	D50 (mm)	Small Cobbles (%)	Very Coarse Gravel (%)	Coarse Gravel (%)	Medium Gravel (%)	Fine Gravel (%)	Very Fine Gravel (%)	Very Coarse Sand (%)	Coarse Sand (%)	Medium Sand (%)	Fine Sand (%)	Very fine Sand (%)	Very Coarse Silt (%)	Coarse Silt (%)	Medium Silt (%)	Fine Silt (%)	Very Fine Silt (%)	Total Clay (%)
BF1	0.04	100.0	100.0	97.1	95.8	94.4	93.9	93.6	92.9	92.5	91.7	88.8	80.3	74.0	70.9	26.7	16.1	0.0
BF1	17.50	100.0	100.0	75.0	47.0	28.0	14.0	14.0	14.0	14.0	8.0	8.0	8.0	8.0	0.0	0.0	0.0	0.0
BF1	0.04	100.0	100.0	97.1	95.8	94.4	93.9	93.6	92.9	92.5	91.7	88.8	80.3	74.0	70.9	26.7	16.1	0.0
BF1	17.50	100.0	100.0	75.0	47.0	28.0	14.0	14.0	14.0	14.0	8.0	8.0	8.0	8.0	0.0	0.0	0.0	0.0
BF1	27.00	100.0	95.0	60.0	18.0	6.0	3.0	3.0	3.0	3.0	0.0	0.0	0.0	0.0	0.0	0.0	0.0	0.0
BF2	0.07	100.0	100.0	99.1	95.7	93.7	92.1	91.9	89.0	85.1	79.7	68.3	55.6	48.3	45.7	23.5	10.7	0.0
BF2	15.00	100.0	100.0	90.0	53.0	29.0	23.0	21.0	21.0	21.0	21.0	21.0	21.0	21.0	0.0	0.0	0.0	0.0
BF2	34.00	100.0	91.0	39.0	6.0	3.0	2.0	2.0	2.0	2.0	2.0	2.0	2.0	2.0	0.0	0.0	0.0	0.0
BF3	0.04	100.0	100.0	100.0	99.9	99.6	99.5	99.5	98.8	97.8	94.6	87.1	73.4	65.6	62.5	38.4	17.4	0.0
BF3	29.50	100.0	95.0	59.0	23.0	6.0	6.0	6.0	6.0	6.0	1.0	1.0	1.0	1.0	0.0	0.0	0.0	0.0
BF3	29.00	100.0	97.0	57.0	20.0	8.0	4.0	4.0	4.0	4.0	0.0	0.0	0.0	0.0	0.0	0.0	0.0	0.0
BF4	0.06	100.0	100.0	100.0	99.9	99.8	99.7	99.6	98.0	96.6	93.7	84.2	69.5	59.8	56.3	30.7	12.6	0.0
BF4	24.00	100.0	98.0	79.0	21.0	0.0	0.0	0.0	0.0	0.0	0.0	0.0	0.0	0.0	0.0	0.0	0.0	0.0
BF4	18.00	100.0	95.0	69.0	43.0	26.0	19.0	19.0	19.0	19.0	0.0	0.0	0.0	0.0	0.0	0.0	0.0	0.0
BF5	24.50	100.0	93.0	69.0	27.0	9.0	7.0	7.0	7.0	7.0	7.0	7.0	7.0	7.0	0.0	0.0	0.0	0.0
BF5	32.00	100.0	91.0	49.0	15.0	2.0	0.0	0.0	0.0	0.0	0.0	0.0	0.0	0.0	0.0	0.0	0.0	0.0
BF6	0.04	100.0	100.0	98.5	98.5	98.4	98.4	98.4	97.9	96.7	94.8	89.4	79.9	69.8	65.2	37.1	15.5	0.0
BF6	20.00	100.0	99.0	75.0	38.0	17.0	13.0	12.0	12.0	12.0	0.0	0.0	0.0	0.0	0.0	0.0	0.0	0.0
BF6	0.04	100.0	100.0	100.0	96.9	95.6	94.0	93.8	92.0	90.5	87.9	84.2	77.5	72.5	69.8	30.9	16.0	0.0
BF6	19.50	100.0	96.0	79.0	38.0	14.0	9.0	6.0	6.0	6.0	0.0	0.0	0.0	0.0	0.0	0.0	0.0	0.0
BF6	43.50	100.0	74.0	29.0	8.0	3.0	1.0	1.0	1.0	1.0	0.0	0.0	0.0	0.0	0.0	0.0	0.0	0.0

APPENDIX C

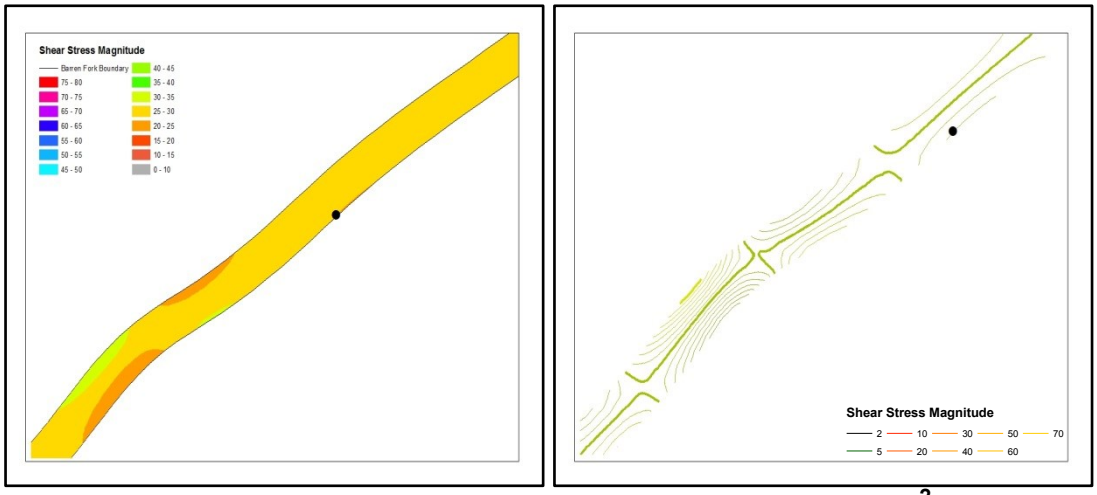

Site BF1 – Magnitude of applied shear stress (N/m^2)

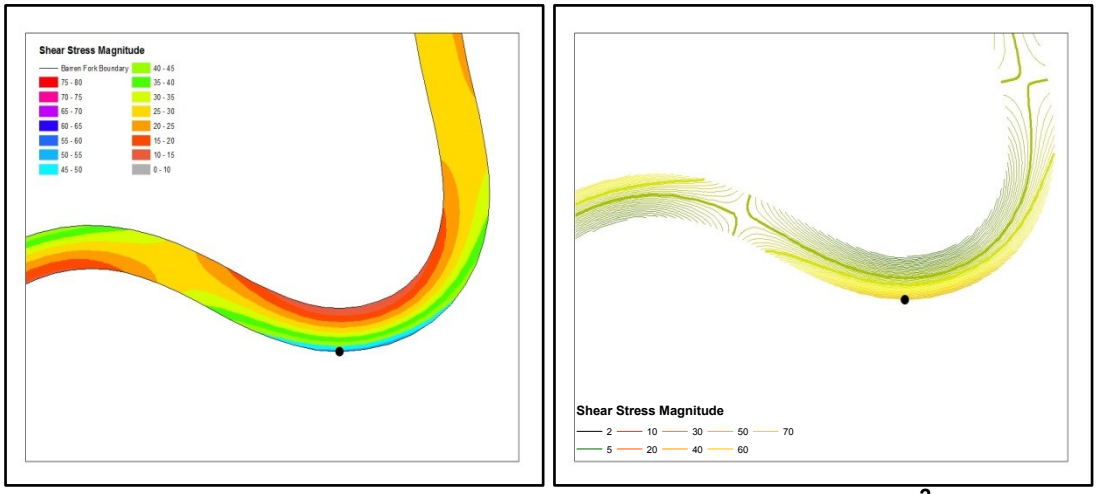

Site BF2 – Magnitude of applied shear stress (N/m^2)

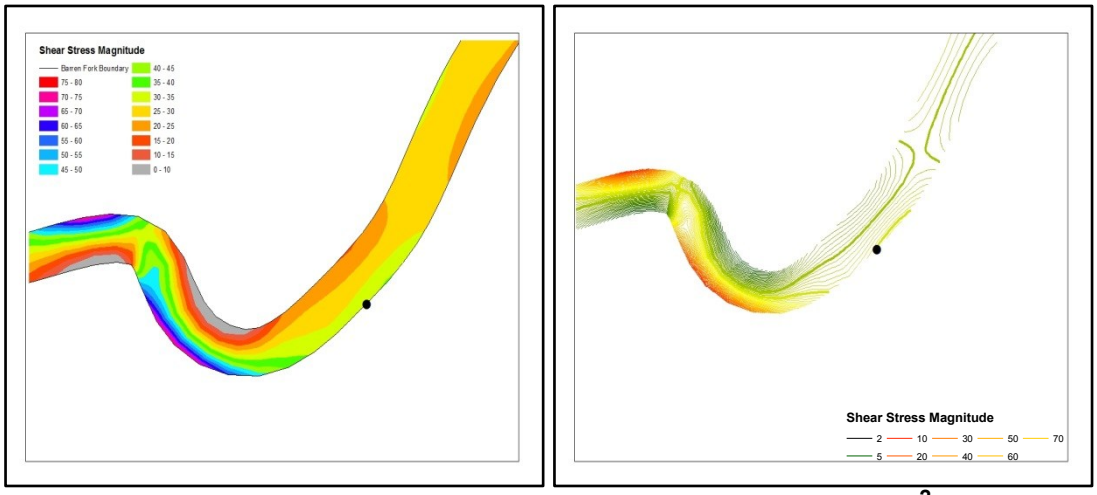

Site BF3 – Magnitude of applied shear stress (N/m^2)

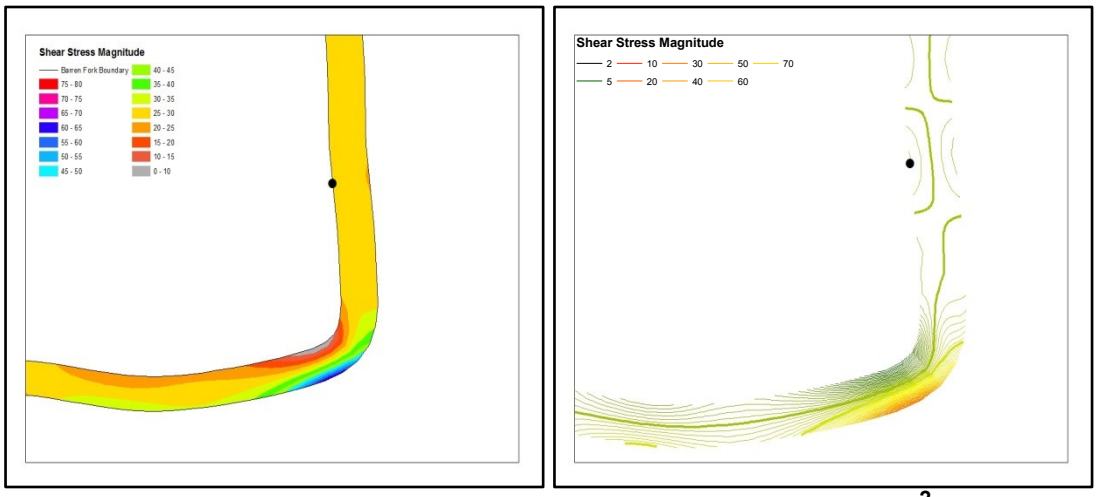

Site BF4 – Magnitude of applied shear stress (N/m^2)

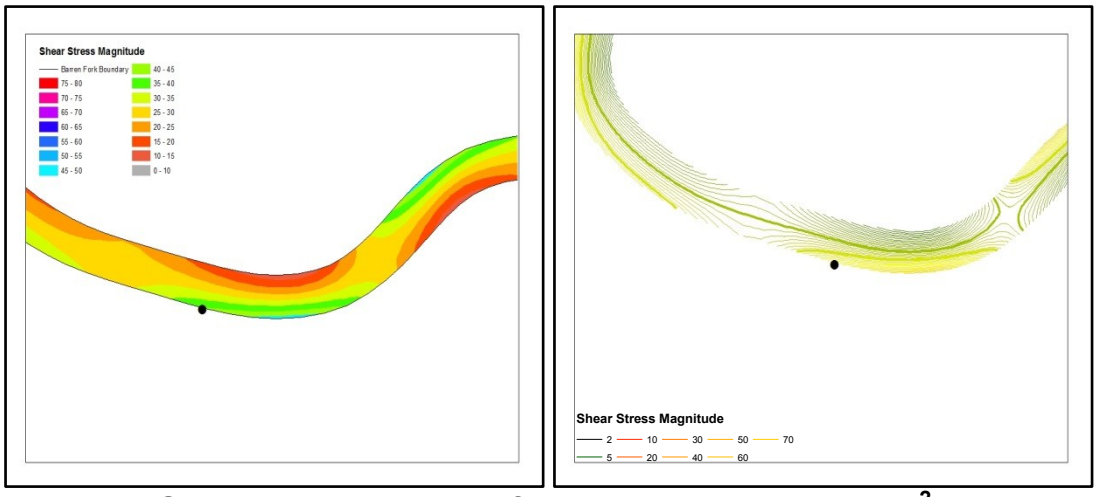

Site BF5 – Magnitude of applied shear stress (N/m^2)

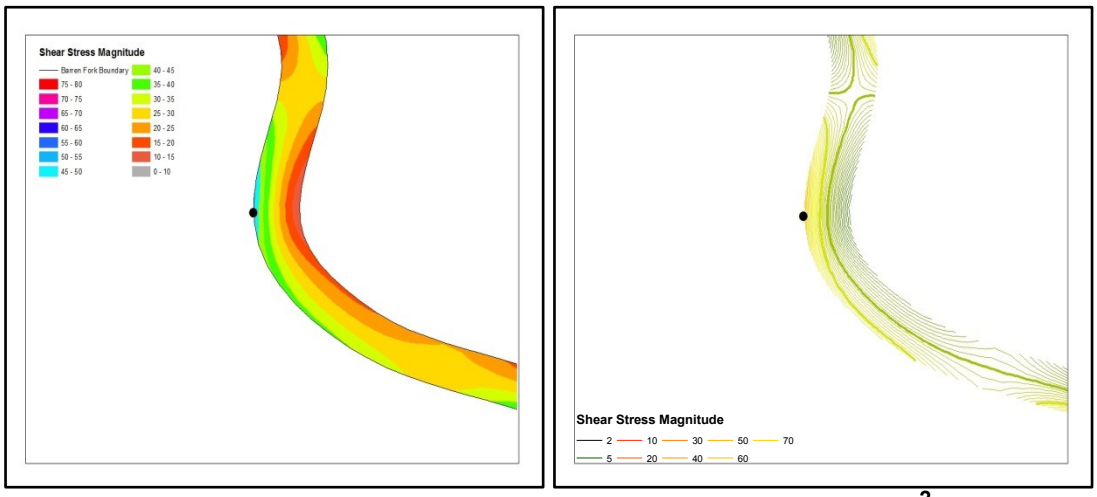

Site BF6 – Magnitude of applied shear stress (N/m^2)

APPENDIX D

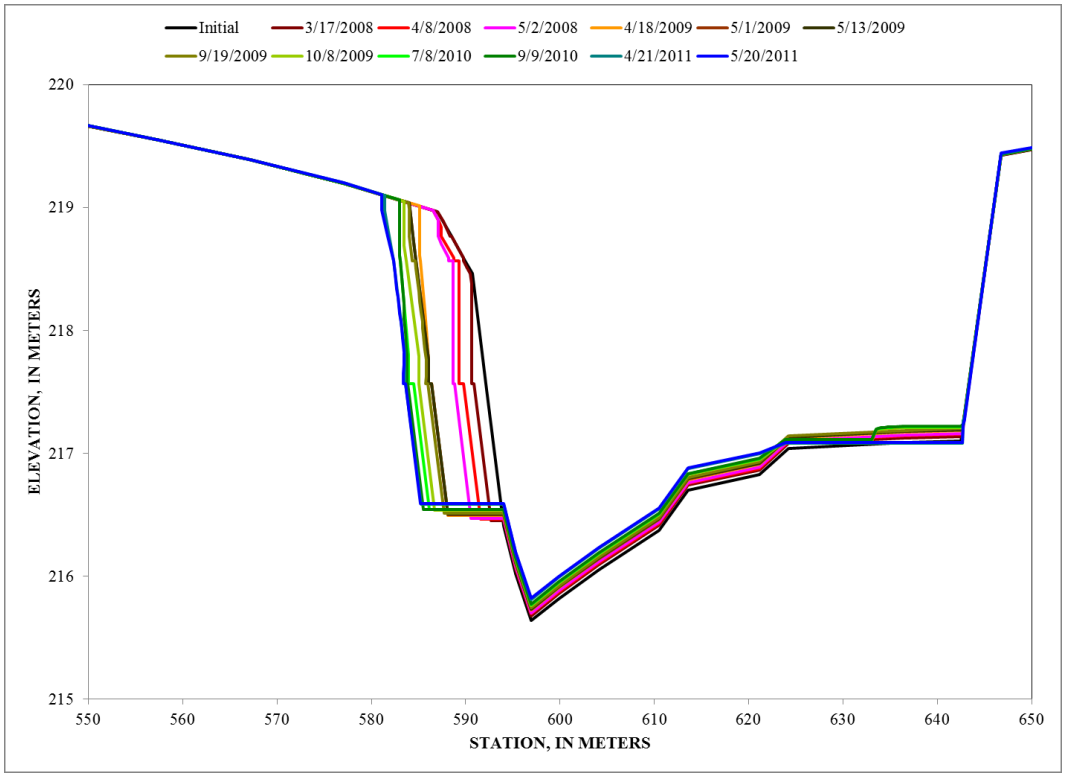

Site BF1

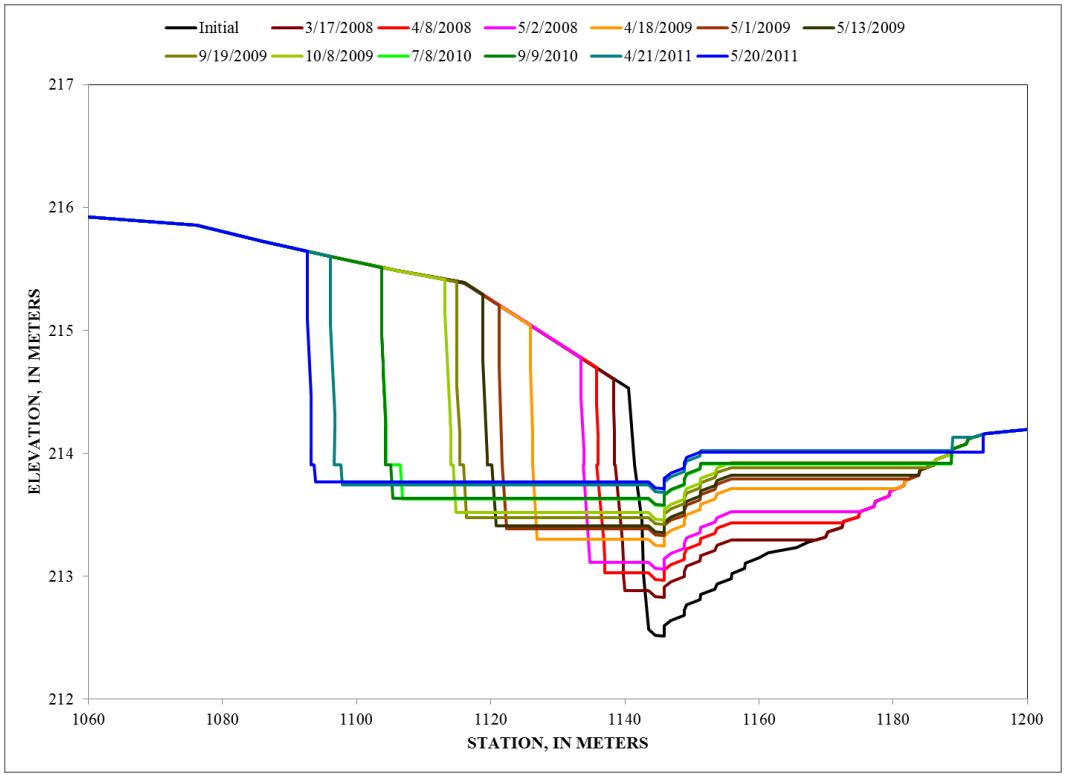

Site BF2

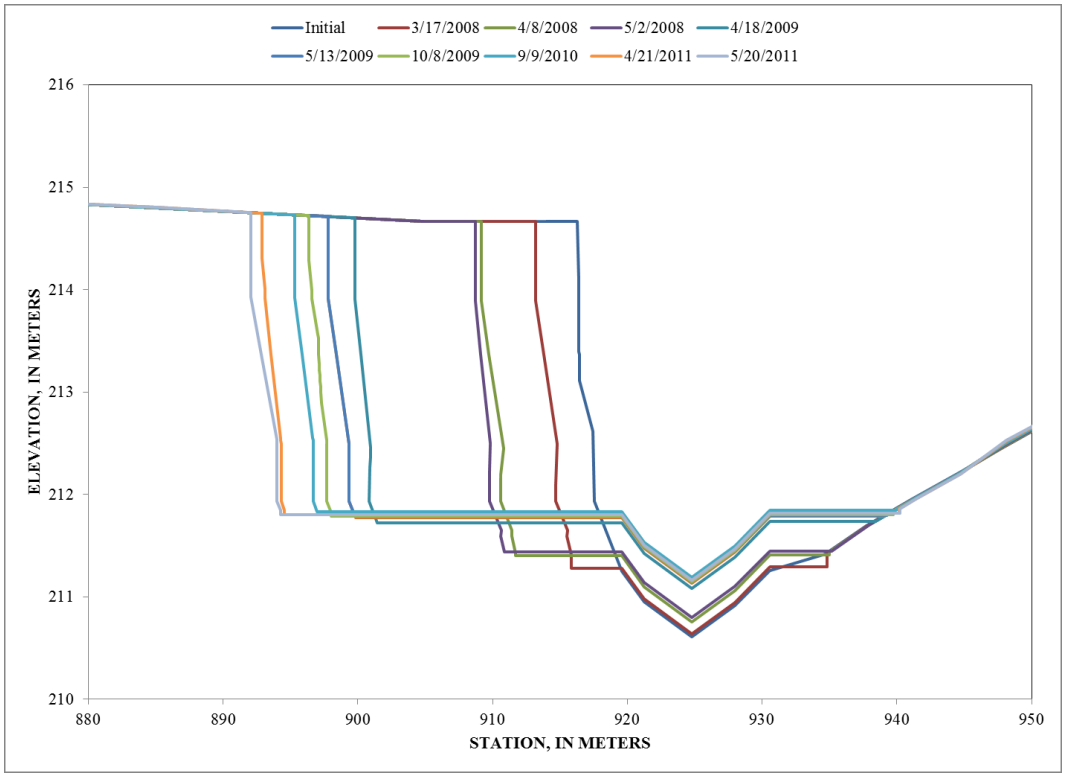

Site BF3

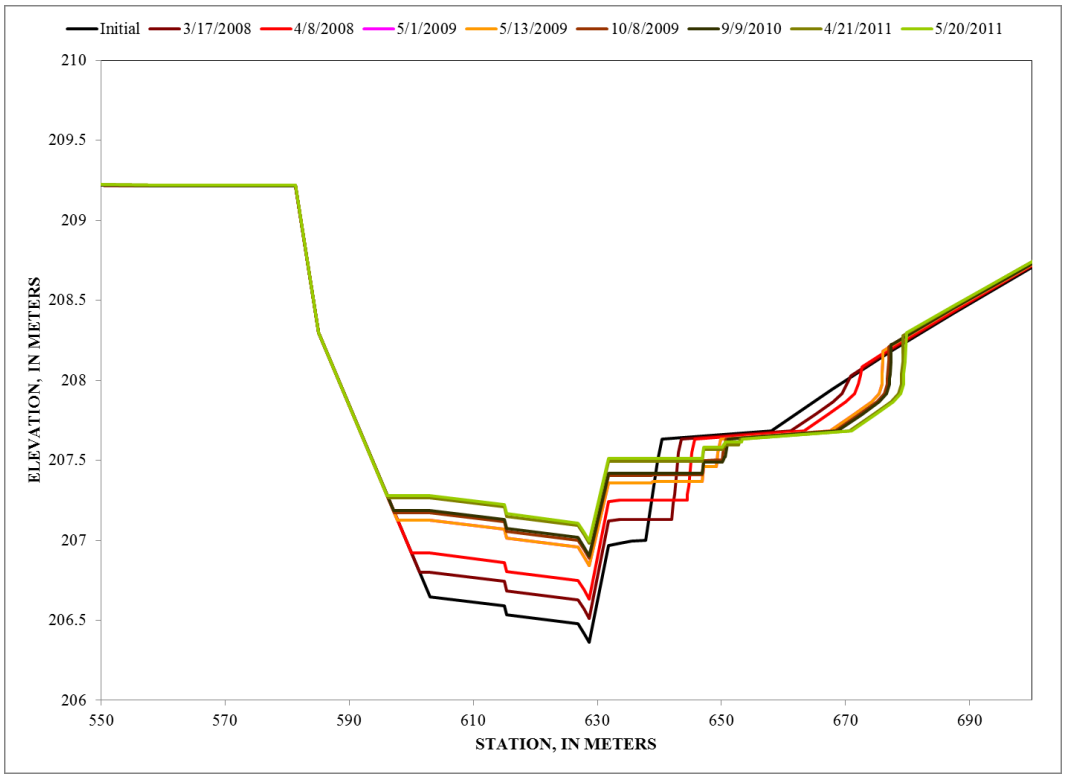

Site BF4

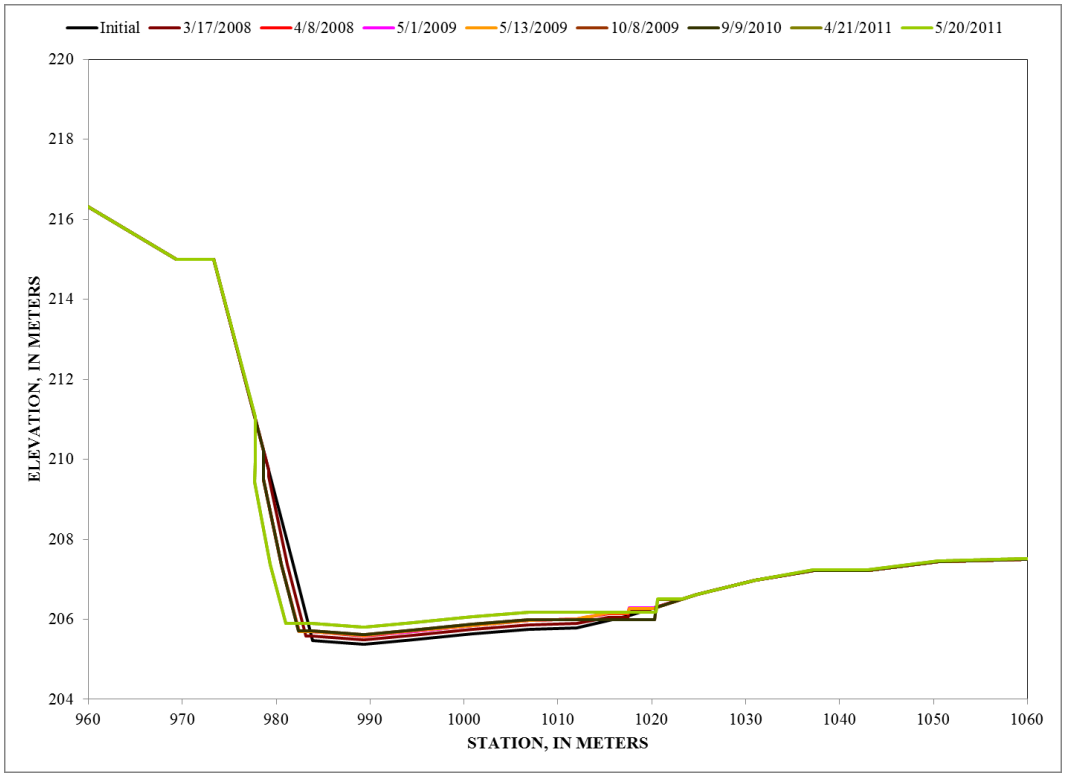

Site BF5

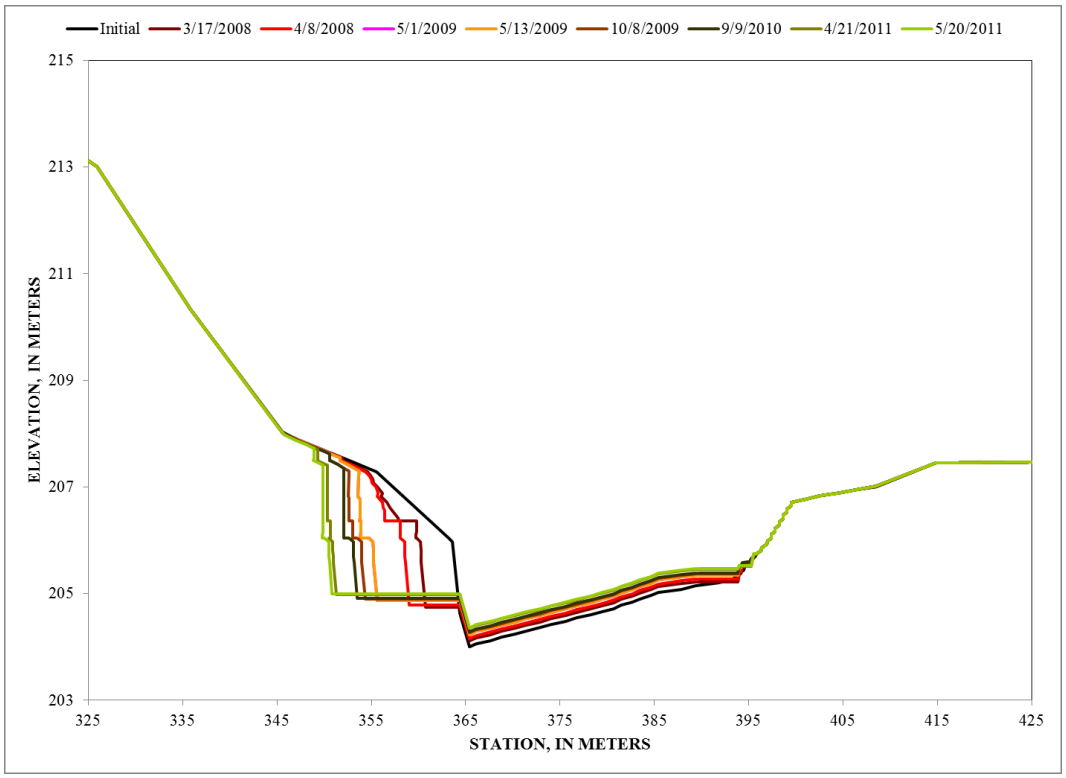

Site BF6

VITA

Erin Rebecca Daly

Candidate for the Degree of

Master of Science

Thesis: EVALUATION OF THE CONSERVATIONAL CHANNEL EVOLUTION AND POLLUTANT TRANSPORT SYSTEM (CONCEPTS) APPLIED TO COMPOSITE STREAMBANKS IN THE OZARK HIGHLANDS ECOREGION

Major Field: Biosystems and Agricultural Engineering

Biographical:

Education: Completed the requirements for the Master of Science in Biosystems and Agricultural Engineering at Oklahoma State University, Stillwater, Oklahoma in December, 2012.Completed the requirements for the Bachelor of Science in Biosystems Engineering at Clemson University, Clemson, South Carolina in May, 2010.

Experience: Research and teaching assistant at Oklahoma State University; Research Assistant at Clemson University; Scholar Intern at the NOAA National Marine Fisheries Service Pacific Islands Regional Office; Ernest F. Hollings Scholar, Class of 2008; Engineering Ambassador at Clemson University; Research Assistant at the Belle W. Baruch Institute of Coastal Ecology and Forest Science.

Professional Memberships: American Society of Agricultural and Biological Engineers.